SSRG International Journal of Civil Engineering
ISSN: 2348-8352/ https://doi.org/10.14445/23488352/IJCE-V12I7P117

Volume 12 Issue 7, 200-227, July 2025

Original Article

Simulation of Vibration Transmission through Soil Medium: Modelling Peak Particle Velocity Attenuation using Multi-Parameter Analysis

Kioko, Paul Christopher Kimali[1], Sylvester Abuodha[2], John Mwero[3], Zacharia Kuria[4]

[1,2]*Department of Civil and Construction Engineering, Nairobi, Kenya.*
[3]*Department of Structural and Construction Engineering, Nairobi, Kenya.*
[4]*Department of Geology, University of Nairobi, Nairobi, Kenya.*

[1]*Corresponding Author : engkimalikioko@gmail.com*

Received: 15 May 2025 Revised: 18 June 2025 Accepted: 17 July 2025 Published: 31 July 2025

Abstract *- Ground motion from freight rail transport can significantly impact nearby structures, necessitating an understanding of vibration transmission through soil. This study investigates vibration attenuation in compliance with the International Organization for Standardization. (2005). Mechanical vibration—Ground-borne noise and vibration arising from rail systems—Part 1: General guidance (ISO 14837-1:2005); Geneva, Switzerland: ISO [24] using triaxial ADXL-345 accelerometers [5,9] and I²C protocol for data logging at 8-metre intervals from the rail line. Ground vibration was measured as Peak Particle Velocity (PPV), derived from acceleration data via double integration in Python. The highest recorded PPV was 8.065 mm/s at 8 metres, attenuating to 2.466 mm/s at 32 metres with significant decay below 15 Hz frequency. A multi-parameter exponential model analyzed PPV attenuation considering soil properties like California bearing ratio, stiffness, shear strength, density and Poisson's ratio. Field results aligned with model predictions, showing PPVs within recognized safety standards such as EuroCode 8[17]. Vibrations were below damage thresholds, with safety assured beyond 100 metres from the rail line. This study enhances understanding of soil dynamics, providing a predictive model for PPV attenuation that aids in designing resilient structures and mitigating vibration-induced damage. Future research should incorporate machine learning to improve predictive accuracy, advancing infrastructure resilience and compliance with global standards.*

Keywords *- ADXL-345 accelerometers, Freight rail transport, Ground motion, Peak particle velocity, Vibration transmission.*

1. Introduction

Ground motion induced by external factors, such as freight rail transport, can significantly impact nearby residents and structures constructed in close proximity to the vibration source. Recent advances in ground vibration monitoring, as evidenced by studies such as [4], enable the precise prediction and mitigation of vibrations caused by freight rail transport. These vibrations, occurring primarily in the low-frequency range up to 15 Hz, are influenced by soil and track flexibility, as explained by [3].

Vibrations' implications for structural integrity, damage, and well-being, highlighted by [22], call for interventions. International standards and codes such as Australian Standards-ASCA 23-1967 and International Organization for Standardization (2005), *Mechanical vibration—Ground-borne noise and vibration arising from rail systems—Part 1: General guidance* (ISO 14837-1:2005). Geneva, Switzerland: ISO [24] provide vital guidelines.

Triaxial accelerometers are used to assess the vibration attenuation with distance from the source, which is crucial for controlling and preventing vibrations in railway transportation, as shown by [13]. This study aimed to understand the impact of vibrations on residents near rail lines and identify mitigation measures using triaxial accelerometers.

In summary, recent advancements in monitoring and mitigating ground vibrations from freight rail transport are crucial for enhancing the structural integrity and preserving well-being. Understanding train-induced vibrations and their effects on structures and individuals is essential for a resilient infrastructure and urban planning. Soil serves as a critical interface between structures and external forces, influencing their dynamic responses and long-term stability.

Vibration transmission through soil can have significant implications for the design and performance of infrastructure systems as well as for environmental management practices. The Ground vibration due to passing trains was measured as peak particle velocity(mm/s), which is defined as the maximum instantaneous velocity value of a soil particle reached during the concentric phase at a given load of the train passes.

Globally, similar patterns are observed in cities across Africa, Asia and Latin America, where infrastructure expansion outpaces the integration of vibration risk assessment in design codes and regulatory frameworks.

Despite growing awareness, most predictive models for ground vibration attenuation remain oversimplified and inadequately suited to developing contexts. Existing models often focus on single-parameter relationships—typically distance from the vibration source—while neglecting critical soil characteristics such as stiffness, density, and moisture variability. Furthermore, these models are largely region-specific, derived from studies in North America or Europe, with limited calibration for diverse geotechnical conditions found in Sub-Saharan Africa.

Key limitations in current predictive approaches include:

Oversimplified modeling-Reliance on exponential decay models that ignore the role of multiple interacting soil properties.

Poor local calibration- A lack of empirical data from Sub-Saharan settings makes global standards (e.g., ISO 14837, Caltrans guidelines) less applicable.

Neglect of near-field effects-Many models underestimate vibration amplitudes within 0–40 metres of rail lines—zones that often contain informal settlements or critical infrastructure.

Unaddressed resonance hazards-Potential soil–structure resonance effects remain largely ignored.

Serviceability disconnects-There is limited attention to functional performance and occupant discomfort, even when structural damage is absent.

Regulatory void-Most African countries lack formal vibration exposure standards, making it difficult to enforce design safety.

Limited use of real-time sensor data-Few studies leverage low-cost, triaxial accelerometers for dynamic monitoring or model calibration.

The table below shows the gaps and limitations of existing studies, which this study endeavours to address:

Table 1. Empirical & Numerical Models

Study	Model Type	Excitation Type	Strengths	Limitations	Relevance
Caltrans (2002)	Empirical	Rail & Road	Defines baseline PPV limits	Ignores soil type variability	Useful for setting vibration thresholds
Kouroussis et al. (2013/14)	Numerical (FEM/BEM)	Harmonic Rail Load	Captures full wave propagation	Complex & location-dependent	Key for SSI modeling
Jingjing Hu et al. (2018)	Empirical	Metro/Freight	City-scale PPV trends	Lacks soil-specific calibration	Aids urban decay curve fitting
Numerical Modelling of Building Vibrations (2017)	Numerical	Rail Loads	Simulates structural response	No in-situ validation	Useful for building response analysis
Madshus et al. (1996)	Semi-Empirical	Train-Induced	Focus on soil damping, SSI	Based on Nordic conditions	Baseline for soil damping calibration
Ribes-Lario et al. (2017)	Standards-Based	Continuous Rail	Aligns with Eurocode/ISO	Not location-adapted	Guidance for regulatory thresholds
Dong-Soo Kim et al. (2000)	Lab-Experimental	Impulse	Focus on stratified soils	Lab-based, lacks scale-up	Validates wave speed, damping layers
Mohammad et al. (2018)	Sensor-Based Empirical	Freight Rail	Field sensor validation	Does not propose a full model	Matches current sensor methodology
Mobaraki et al. (2022)	Sensor-Based	Freight Rail	Real-time wireless sensors	Limited African application	Supports low-cost sensor adoption
Islam et al. (2020)	Sensor + Arduino	Rail	Tracks wheel & rail vibrations	Limited to the rail element	Shows MEMS feasibility
Erkal Aykut et al. (2010)	Numerical	Rail/Seismic	SSI and amplification effects	Uniform soil assumptions	Foundation for resonance analysis

Sodev (1975)	Early Empirical	Blasting	Origin of empirical attenuation	Outdated	Historical foundation
Golitsin (1912)	Theoretical	Seismic	Introduced wave theory	No application model	Foundational wave mechanics

Table 2. Vibration Effects: SLS vs ULS ISO 2631-2:2003 — Mechanical vibration and shock — Evaluation of human exposure to whole-body vibration-Part 2: Vibration in buildings (1 Hz to 80 Hz) [23]

Vibration Parameter	Typical Threshold	Effect on Serviceability (SLS)	Effect on Structural Integrity (ULS)
Low-Frequency Vibrations	≤15 Hz	- Perceptible motion- Disturbed occupants- Cracking of finishes- Misalignment of doors/windows	- Resonance with structure- Fatigue in connections- Progressive structural weakening
Peak Particle Velocity (PPV)	0.3 – 0.5 mm/s	- Human discomfort- Building vibrations perceptible	- No damage expected
	1 – 5 mm/s	- Annoyance- Sensitive equipment affected (e.g., medical/labs)	- Possible cracking in masonry or old structures
	>5 – 10 mm/s	- Loss of function in vibration-sensitive areas	- Minor to moderate structural damage (especially in ULS-weak elements)
	>10 mm/s	- Severe disruption	- Major cracking or displacement of elements; possible structural failure

Table 3. Alignment of research gaps with study objective

Research Gap	Alignment with Objective
1. Lack of local calibration for soil-vibration behavior	Objective: To determine the geotechnical properties of the soil medium
2. Inadequate treatment of near-field effects (0–40 m)	Objective: To establish characteristics of ground vibration propagation
3. Neglect of multi-parameter inputs (soil, structure, source) in predictive models	Objective: To simulate vibration transmission through the soil medium
4. No linkage between attenuation curves and building serviceability thresholds	Objective: To establish propagation characteristics and simulate structural implications
5. Insufficient consideration of soil-structure resonance risks	Objective: To simulate vibration transmission and assess resonance potential
6. Lack of region-specific vibration thresholds & regulatory data	Cross-cutting (supports policy application of all objectives)

This study addresses these gaps by developing and validating a multi-parameter exponential attenuation model for Peak Particle Velocity (PPV) based on real-time field data from ADXL-345 accelerometers. By integrating multiple geotechnical parameters—such as soil stiffness, shear strength, California Bearing Ratio (CBR) and density—into the modeling framework, the study seeks to improve predictive accuracy and enhance infrastructure resilience in regions with high vulnerability but limited resources. The work also aims to support future efforts in establishing localized vibration exposure thresholds and practical design guidelines for developing economies.

The research problem addressed in this study revolves around the need to accurately predict and mitigate the attenuation of Peak Particle Velocity (PPV) as vibrations propagate through the soil medium. The ability to quantify PPV attenuation is crucial for assessing the potential impact of vibrational loads on structures, determining suitable locations for construction projects, and implementing effective measures for controlling vibrations in sensitive environments.

A thorough review of the relevant literature revealed a wealth of research on soil dynamics, vibration analysis, and existing models for predicting PPV attenuation. Previous studies have explored various factors that influence soil behavior and their effects on vibration transmission. However, many existing models focus on single variables and may not fully capture the complex interplay between multiple soil parameters.

Objective: Simulation of vibration transmission through the soil medium

Understanding the intricate dynamics of vibration propagation through soil is indispensable for a multitude of engineering endeavors. By assessing construction impacts to forecast seismic event repercussions, precise simulations of vibration behavior provide invaluable insights for planning and mitigation strategies.

The propagation of ground vibrations from freight trains poses growing risks to structural serviceability, especially in rapidly urbanizing areas like Nairobi Metropolis in Kenya. The literature surveyed contributes foundational and recent insights into how vibrations transmit through various soils, decay with distance and impact infrastructure—directly supporting the objective of predicting and mitigating vibration risks from rail operations.

This study explores the simulation of vibration propagation in soil, with a specific focus on modelling the exponential attenuation of vibrational waves. This phenomenon, characterized by a swift reduction in vibrational energy over distance, is influenced by various soil parameters. Our simulation framework centers on depicting the peak particle velocity, distance travelled, and soil factors, offering a holistic understanding of vibration attenuation dynamics.

Using an exponential model for predicting Peak Particle Velocity (PPV) values offers a great advantage in providing vibration patterns and trends in this study, according to [26, 29], which include the following:

Flexibility to capture non-linear relationships- Exponential models can capture non-linear relationships more effectively than linear models such as Ordinary Least Squares (OLS) regression, such that, since the relationship between distance and PPV exhibits exponential growth or decay, an exponential model would provide the desired fit. Better representation of the physical phenomena.

In this study involving physical processes, the relationship between the variables ppv and distance follows exponential patterns as in wave propagation phenomena, such as seismic waves, where the attenuation of energy often follows an exponential decay with distance. Thus, the use of an exponential model better represents this phenomenon.

1.1. Interpretation of the Parameters

Even where parameters in exponential models may not have direct interpretations in terms of units, they often have intuitive interpretations related to the underlying process and vibration attenuation in this case. In the exponential decay model, the decay rate parameter represents the rate at which the ppv quantity decays over time and distance, as demonstrated in this study.

1.2. Accurate Extrapolation

Exponential models provide more accurate extrapolations beyond the observed range of data, particularly in this study, where the relationship continues to follow an exponential pattern. This was particularly useful for predicting the PPV values at distances that were not included in the original dataset.

1.3. Robustness to Outliers

Exponential models are more robust to outliers than linear models, such as OLS regression. Outliers that deviate significantly from the overall trend have less influence on the parameter estimation in an exponential model, and this attribute contributes to accurate curve fitting.

1.4. Improved Model Fit

In this study, the relationship between variables was inherently exponential, and using the exponential model resulted in a better fit to the data compared to linear and other models. This leads to more accurate predictions and a better understanding of the underlying processes.

Theoretical justification: In this scientific research field, theoretical justifications for using exponential models are based on fundamental principles and previous empirical findings. In this case, the exponential model aligned well with the established theories and empirical models.

Several research postulations support the adoption of exponential modelling in ground vibration research. These citations provide examples of research studies and literature relevant to the decay of peak particle velocity with distance, which often follows an exponential pattern in various contexts, such as seismic attenuation, ground vibration propagation, blast-induced vibration, environmental impact assessment and structural health monitoring.

1.5. Seismic Attenuation

The textbook [2] discusses seismic attenuation, which often follows an exponential decay pattern with increasing distance from the seismic source.

1.6. Ground Vibration Propagation

The study [26] examines ground vibration propagation from railroad traffic, where the amplitude of vibration typically decays exponentially with the distance from the source.

1.7. Blast-Induced Vibration

The review discusses blast-induced ground vibrations in mining operations, where the decay of the vibration intensity with distance often follows an exponential pattern.

1.8. Environmental Impact Assessment

The study [21] investigated the environmental impact of pile driving activities, including the attenuation of vibration amplitudes with distance, which may exhibit exponential decay behavior.

1.9. Structural Health Monitoring

The review discusses techniques for structural health monitoring, including the analysis of vibration decay rates, which can be modelled using exponential functions.

The number of vibration sensor points was significantly expanded compared with previous studies, ensuring a more comprehensive representation of the vibration profile of the site. By leveraging Python, double integration of acceleration data was conducted from these multiple sensor points, enabling precise determination of the peak particle velocity and enhancing the fidelity of our simulations.

Thereafter, a model was formulated using the peak particle velocity and distance and incorporating the soil attenuation factor, which was validated using other established empirical models, and the results were found to align quite well with them. The established empirical models, which are validated in section 3.2 of this research, include the following:

California Department of Transportation. (2002, February 20). *Technical Advisory on Vibration: TAV-02-01-R9601*. California Department of Transportation [13], where the following equation was postulated to demonstrate that surface waves generated by traffic, trains, and most construction operations tend to attenuate with distance according to the equations as shown below

$$V= V_0(D_0/D)^{0.5}\, e^{\alpha(D0-D)} \quad \text{and} \quad V= V_0(D_0/D)^{k} \qquad (1)$$

Where: V = Peak particle velocity at distance D
V_0 = Peak particle velocity at reference distance D_0
D_0 = Reference distance
D = Distance for which the vibration level needs to be calculated
e = Base of natural logarithm = 2.718281828
k = Soil parameter
α = Soil parameter

The soil parameter α was determined by simultaneous vibration measurements at a minimum of two different distances from the vibration source, providing a soil factor of 0.080 and yielding the same simulation results as our model.

According to the California Department of Transportation Technical Advisory on Vibration [13], the maximum vibration levels were 7 mm/s at 7metres from the vibration source, stabilizing at 0.3 mm/s at 100metres from the vibration source.

According to the advisory,0.3 mm/s is the threshold of perception and is unlikely to cause any damage type, while 5 mm/s is considered unpleasant and unacceptable and has the potential to cause "architectural" damage and minor structural damage.

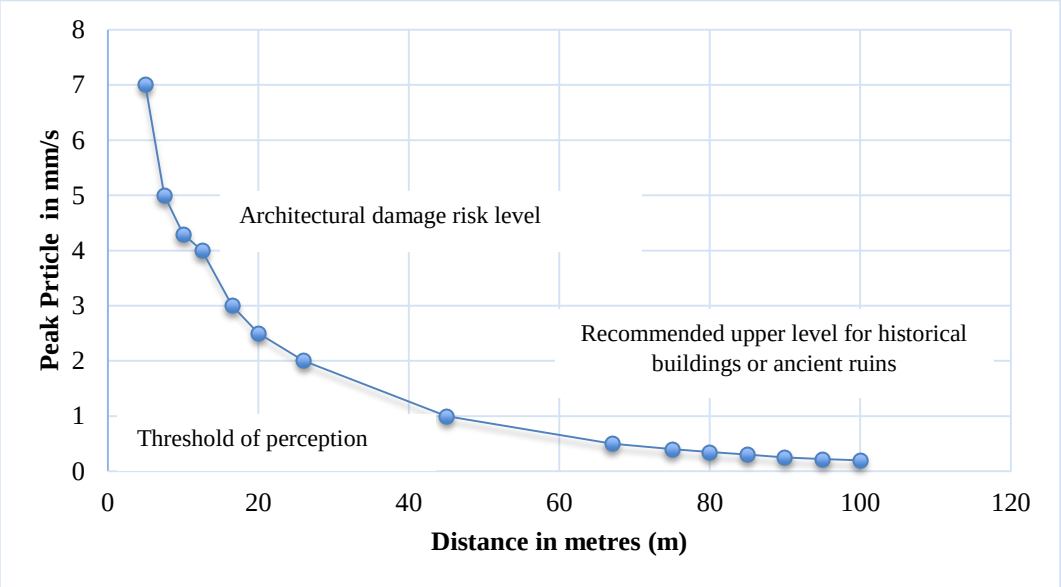

Fig. 1 Maximum Train Vibration Levels vs. Distance
Source: California Department of Transportation. (2002, February 20). *Technical Advisory on Vibration: TAV-02-01-R9601* [13]

The insights from this model align well with the focus on predicting PPV attenuation trends for PPV.
It is useful in complementing this model by offering standard attenuation methodologies to validate these predictions.

- Dong-Soo Kim, Jin-Sun Lee *et al*, (2000). Propagation and attenuation characteristics of various ground vibrations. *Soil Dynamics and Earthquake Engineering*, 19(2), 115–126. https://doi.org/10.1016/S0267-7261(00)00002-6 [14]

Equally, the other empirical model explored was that of a study by Dong-Soo Kim, Jin-Sun Lee *et al* (2000), where propagation and attenuation characteristics of various ground vibrations were computed as per equation

$$w2=w1\,(\frac{r1}{r2})^{n}e^{-\alpha(r2-r1)} \qquad (2)$$

Where $w_1$and w_2 are the vibration amplitudes at distances $r_1$and r_2 from the rail source of vibration, respectively, and the material damping coefficient obtained is 0.08.

The research is relevant in that it focuses on soil dynamics and vibration transmission.

It contributes to understanding soil properties without a specific focus on PPV as the only measure for attenuation trends.

- A H Mohammad, A Yusoff et al (2018). Ground Vibration Attenuation Measurement using Triaxial and Single Axis Accelerometers [1]

The other empirical model compared with our model was by [1], which is stated as PPV;

$$y=3.2833x^{-1.371} \quad (3)$$

Where y is the peak particle velocity and x is the distance.

The peak particle velocity here ranged from10mm/s at the vibration source to 0.3 mm/s at 32metres from the vibration source.

A similar model was done by [14] with the following graphical trend in Figure 2.

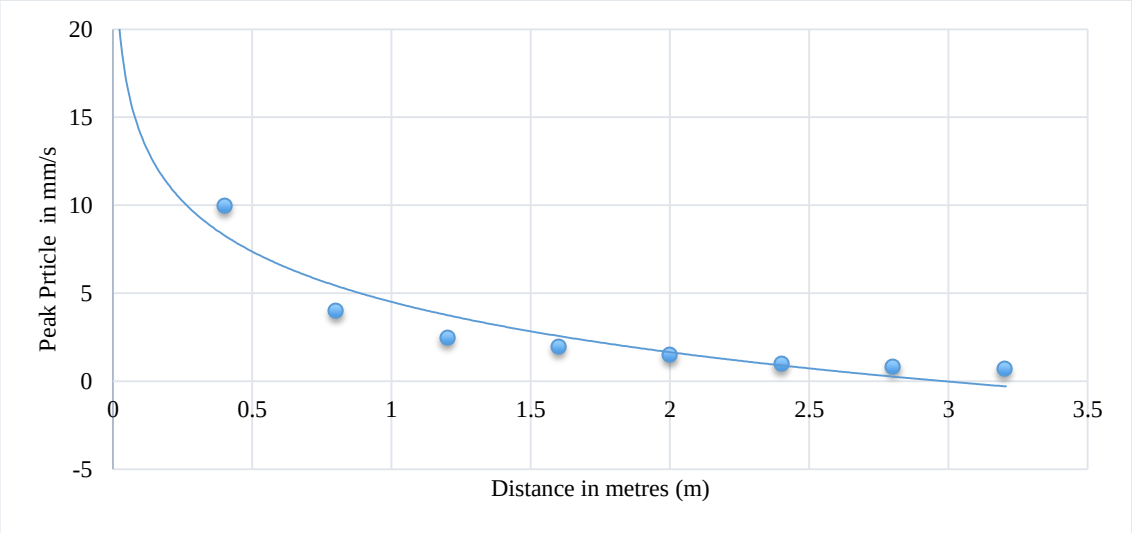

Fig. 2 Peak particle velocity vs distance from the train source

Source: Dong-Soo Kim, Jin-Sun Lee et al (2000). Propagation and attenuation characteristics of various ground vibrations [16]

This study is relevant to this work as it examines vibration attenuation due to transportation activities, including rail transportation-induced vibration. Comparatively, it is useful for broader insights into attenuation behavior but may not be directly aligned with a focus on multi-parameter soil analysis.

- Jingjing Hu,Yi Luo,Ke, Z., Liu, P., & Xu, J. (2018) [25]. Experimental study on ground vibration attenuation induced by viaduct. Proceedings of the Institution of Mechanical Engineers, Part F: Journal of Rail and Rapid Transit, 232(10), 2421–2432. https://doi.org/10.1177/1461348418765949

Also, Jingjing Hu, Yi Luo et al, 2018(Pg11) [25] modelled the ppv that ranged from 5 mm/s at the vibration source to 0.2 mm/s at 60 metres from the vibration source. According to Jingjing Hu, Yi Luo et al 2018 [25], the propagation characteristics of vibrations generated by various vibration sources may be dependent on the type of generated waves, which can be assessed by measuring the particle motions. According to the literature analysis, the magnitude of the dynamic load transmitted to the ground by the pier is mainly affected by the train's running speed and axle weight. After the vibration wave is transmitted to the soil through the pier, it is converted into a ground vibration problem purely under the point-source excitation condition. This was similar to the vibration effect induced by blasting in the middle and far regions. In fact, the propagation medium of blasting vibration and pier vibration caused by wagons is both rock and soil masses, and the vibration of the medium near the protected object is elastic vibration. The research explores vibration propagation and attenuation trends, focusing on multi-factor influences like soil composition and vibration frequency. Comparatively, it aligns directly with this multi-parameter approach and is a key reference for comparative validation.

- Sodev, B. (1975). A new approach to the prediction of ground vibrations from blasting. *International Journal of Rock Mechanics and Mining Sciences*, 12(3), 255–266. https://doi.org/10.1016/0148-9062(75)90013-5.

This seminal work laid the groundwork for the use of the Sodev formula in predicting and analyzing ground vibration levels associated with blasting and construction activities. The modified Sodev formula for predicting the relationship between Peak Particle Velocity (PPV) and distance is attributed to a study by Sodev in the context of vibration attenuation related to blasting and construction activities. The original form of this empirical equation is often associated with the work done in the 1960s by Sodev, specifically related to ground vibrations generated by blasting operations.

Here is how it is typically attributed:

Sodev, N. (1967). "Attenuation of ground vibration due to blasting." Bulletin of the International Association of Engineering Geology, 1(2), 117–122.

This reference is often used in vibration analysis for construction and mining projects, particularly focusing on the attenuation of ground vibration with distance. The relationship between PPV and the distance to the vibration source can be described by the modified Sodev formula, as shown in the equations below.

$$V_{peak}=k'(Q'^{3}/D)^{\alpha'} \quad (4)$$

$$V_{peak}=k'' D^{-\alpha'} \quad (5)$$

$$K'' =k' (Q'^{\alpha'/3}) \quad (6)$$

Where k' and α' are the coefficients related to the local geological conditions, Q' is a comprehensive indicator that considers various factors that affect the source of energy (hereinafter referred to as the energy index), and D is the scaled distance. For the vibration source, two adjustments were applied: the train type and train speed.

In this approach, it was concluded that ground attenuation occurred with increased distance.

It was also concluded that the prediction model was effective under various train speeds, axle loads, and site conditions.

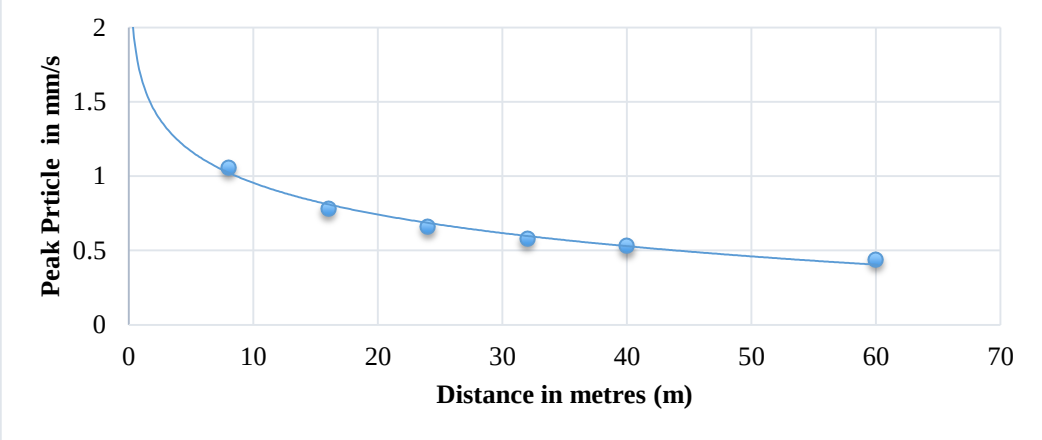

Fig. 3 Power function fitting of PPV under different speeds and weights vs distance to the centre line
Source: Sodev, B. (1975).

This study has a rich historical perspective on vibration modeling.
It, however, has limited applicability due to outdated methodologies that may not align with modern multi-parameter approaches.

- David K. Hein (2006). Mitigation of Highway Traffic-Induced Vibration (Pg9). In Proceedings of the 2006 Annual Conference of the Transportation Association of Canada [13].

In an article by Hein (2006), Mitigation of Highway Traffic-Induced Vibration (Pg9) [13] depicts the effect of soil type on the propagation of vibration.

The vibration velocity is defined as the Peak Particle Velocity (PPV) of the vibratory motion (corresponding to the maximum instantaneous positive or negative vibration velocity) or as the root mean square of the peak velocity. The formula for converting peak velocity (Peak) to root mean square(rms) velocity for a sine wave is given in Equation as

$$\text{rms}=\frac{peak}{\sqrt{2}} \quad (7)$$

The maximum recorded peak particle velocity was 3 mm/s at 3metres from the vibration source to 0.3 mm/s at 100metres from the vibration through soft clay medium.

This study discusses mitigation strategies and vibration propagation in ground media.

It is therefore relevant for understanding vibration control, though primarily focused on highway traffic.

- Numerical Modelling of Building Vibrations due to Railway Traffic: Analysis of the Mitigation Capacity of a Wave Barrier Shock and Vibration Volume 2017, Article ID 4813274, 11 pages https://doi.org/10.1155/2017/4813274.

The next step in the wave propagation path is the transmission from the soil to nearby building foundations. To analyze this process, vertical and horizontal particle velocities and acceleration were analyzed at four points on the foundation slab with increasing distance to the track (A1, A2, A3, and A4) and coincident with the four building columns. The maximum registered values are shown in the Figure below: As shown in the Figure below, the horizontal vibrations are roughly constant along the edge of the slab in terms of both acceleration and velocity. In contrast, the vertical values vary along the edge and are higher in the corners (points 1 and 4) than in the center. Such behavior is expected because the slab presents a very different structural stiffness in each direction (much higher in the horizontal plane than in the vertical plane).

Furthermore, the greater vertical vibration values at the corner points are also explained by the lower structural

constraints of these points when compared to the central ones. A similar analysis was performed to evaluate the transmission of waves from the foundation slab towards the top floor of the building. Therefore, vertical and horizontal vibrations were calculated over the same vertical direction on different floors of the building (A1, B1, C1, and D1). The results are shown in the Figure below.

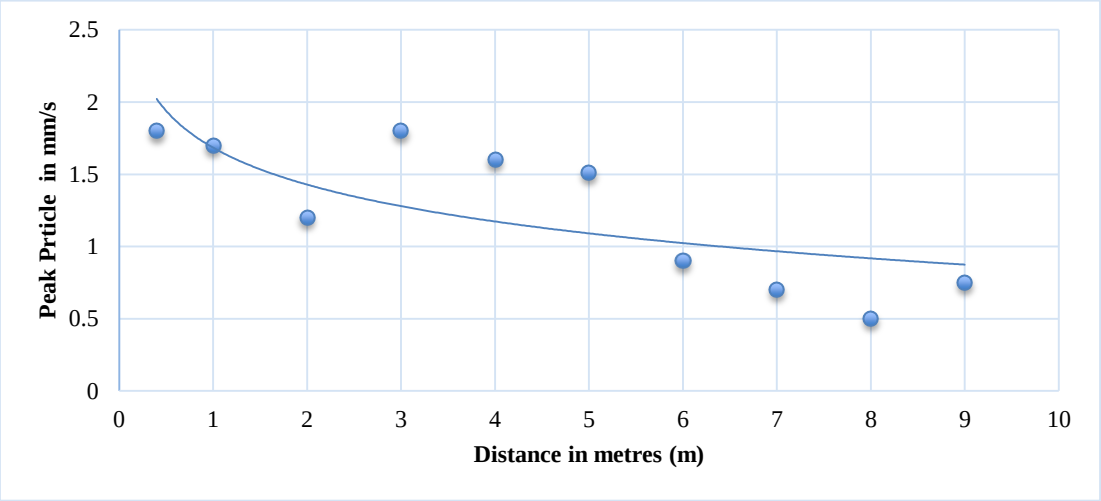

Fig. 4 Soil particle acceleration and velocities at different distances from the track

Source: Numerical Modelling of Building Vibrations due to Railway Traffic: Analysis of the Mitigation Capacity of a Wave Barrier Shock and Vibration Volume 2017, Article ID 4813274, 11 pages https://doi.org/10.1155/2017/4813274

The relevance of this research to this work is that it focuses on vibration mitigation and numerical simulation techniques that analyze wave propagation and attenuation due to railway traffic.

It is highly relevant for understanding soil medium vibration transmission, complementing this modeling approach.

- Georges Kouroussis et al,2014; The 21st International Congress on Sound and Vibration [19]

The study presents typical values, expressed in terms of Peak Particle Velocity (PPV), and obtained from experimental analyses in Belgium for various high-speed train types, as shown in the Figure below, where the solid line represents the curve fit of the type.

$$V = Ay_R^n \qquad \text{Equation 20 of the text.}$$

Where V is peak particle velocity, A is initial amplitude or source factor,y is the correction or soil adjustment factor, R is radial distance from the source and n is attenuation exponent.

The decrease in distance from the track is clearly emphasized, and there is a large discrepancy between ground vibration levels (even for the same type of vehicle), even though the speeds recorded were between 281 and 304 km/h. It was also evident that the vertical component vibration levels were similar to the horizontal vibration levels and were dominant in some cases.

This study focuses more on the analytical model of vibration induced by high-speed trains and not on the soil types.

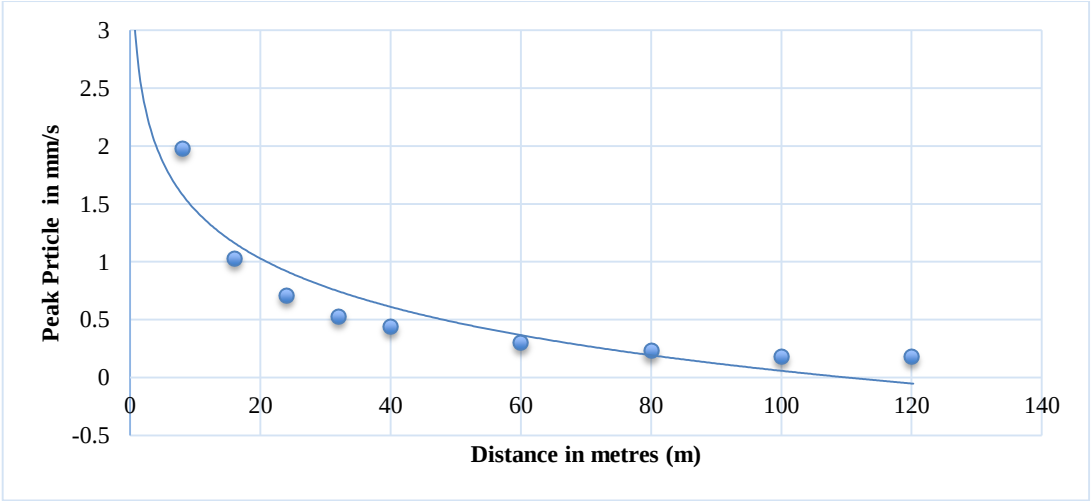

Fig. 5 Peak particle velocity vs distance due to passing of the train

Source: Georges Kouroussis et al, 2014; The 21st International Congress on Sound and Vibration [19]

The relevance of this study is that it extensively discusses numerical modeling of railway-induced vibrations, focusing on soil-structure interaction and multi-parameter analysis. It is closely aligned with this research, offering advanced insights into soil medium modeling, PPV prediction, and multi-parameter considerations like train speed and soil layering.

- Kouroussis, G., Connolly, D, Forde, M. C., Verlinden, O (2013) [19] model

Kouroussis G, Connolly D, Forde MC, Verlinden O (2013) An experimental study of embankment conditions on high-speed railway ground vibrations in Proceedings of the 20th International Congress on Sound and Vibration (ICSV20) International Institute of Acoustics and Vibration, pp. 3034, Proceedings of the 20th International Congress on Sound and Vibration (ICSV20), Bangkok, United Kingdom, 7/07/13[33]. The at-grade ppv is seen to be 1.3 mm/s at an 8metre distance from the vibration source.

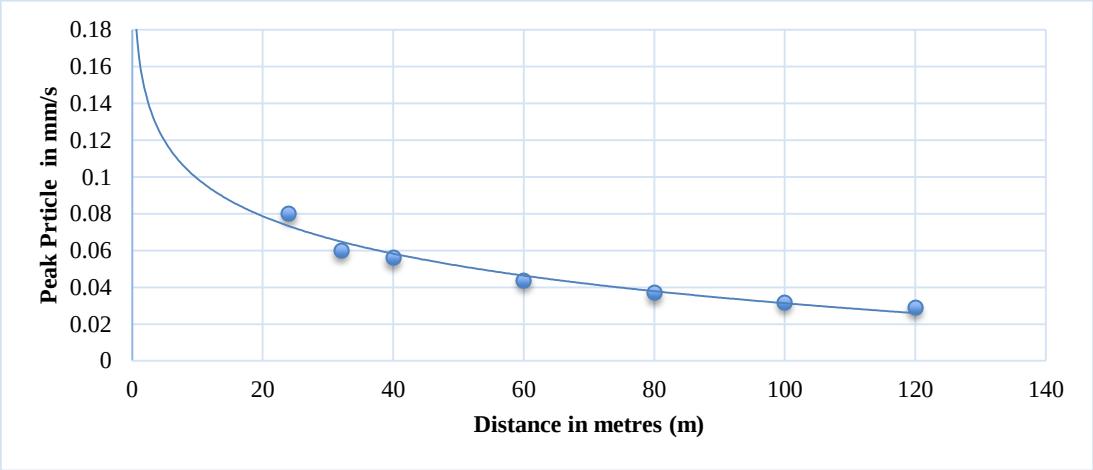

Fig. 6 Influence of soil on vibration-ppv vs distance from track

Source: Kouroussis, G, Connolly, D, Forde, MC, Verlinden, O (2013) [33]

- C. Madshus, B. Bessason and L.Hårvik, Journal of Sound and Vibration, Volume 193, No. 1, 1996 [11]

The model is given as a mathematical function and is adjusted using several factors according to C. Madshus, B. Bessason and L.Hårvik, Journal of Sound and Vibration, Volume 193, No. 1, 1996 [11]

$$\text{Equation } V = F_V F_R F_B = [V_T F_S F_D] F_R F_B \quad (8)$$

Where F_V is the basic vibration function, consisting of a train type specific vibration level V_T for a reference speed and reference distance from the track. F_S is the speed factor, F_D is the distance factor, F_R is the track quality factor, and F_B is the building amplification factor. Another semi-empirical model was developed by M. Bahrekazemi, 2004, Train-induced ground vibration and its prediction, PhD Thesis, Royal Institute of Technology, Sweden [37]. It is based on measurements at four sites in Sweden and incorporates train speed, wheel force, and vibration decay. The measurements included trains with mainly lower speeds, a majority between 70 and 130 km/h, and for speeds outside this range, the relationships established in this model may not be accurate. A Geographical Information System (GIS) was implemented to visualize the particle velocities over an area. This model is classified as a scoping model and is suitable for the preliminary design phase of a project. The mathematical function for the estimation of the particle velocity, Vrms in mm/s, is given as

$$\text{Vrms}=(a.\text{speed}+b)(r/r^0)^{-n} \quad (9)$$

Where a and b are site-specific functions of the wheel force, Frms. The variable speed is the train speed in km/h, r is the distance to the track centerline, r0 is the reference distance (0.85 m), and n is the attenuation factor. M.Bahrekazemi, 2004, Train-induced ground vibration and its prediction, PhD thesis, Royal Institute of Technology, Sweden [37], also developed a more advanced semi-empirical model based on measurements in both Sweden and Finland. It is presented as a MATLAB program with a user interface, with the model divided into four subsystems, each describing a different part of the transmission process. The output from one sub-model is used as the input to the next sub-model. Statistical methods are used to simulate the stochastic nature of the problem. Transfer functions are used to relate vibrations outside a building to vibrations at a point inside the building.

According to C. Madshus, B. Bessason and L. Hårvik, Journal of Sound and Vibration, 193, No. 1, 1996) [11]. The following equation describes the prediction of ground vibrations from the railways:

$$V = V_T * F_D * F_S * F_R * F_B \quad (10)$$

$$V = V_T \times \left(\frac{D}{D_O}\right)^B \times \left(\frac{S}{S_O}\right)^A \times F_R \times F_B \quad (11)$$

Where;

- V = the vibration velocity [*mm/s*].
- V_T = train vibration level perpendicular to the ground (Z direction) at a reference distance D_o, from the center of the railway track and the reference speed S_o [*m/s*].
- F_S is a function of train speed. It can be found using the following equation: $F_S = (S/S_o)^A$, where S is the train speed, and S_0 is the reference speed at which V_T has been measured. A can be between 0.5 and 1.5. In other instances, A = 0.9 is also used.
- F_D is a function of the distance, which could be obtained by $F_D = (D/D_o)^{B,}$

Where D is the distance to the track, and D_0 is the reference distance for which V_T has been measured. B was calculated based on the measurement results.

- F_R is a function of the bedrock. F_R for the bedrock can be 0.7 – 1.3, depending on the type of railway track, whether it is single or double.
- F_B is a function of buildings. For Swedish houses, the resonance is up to three floors, and the F_B is 2 – 3.

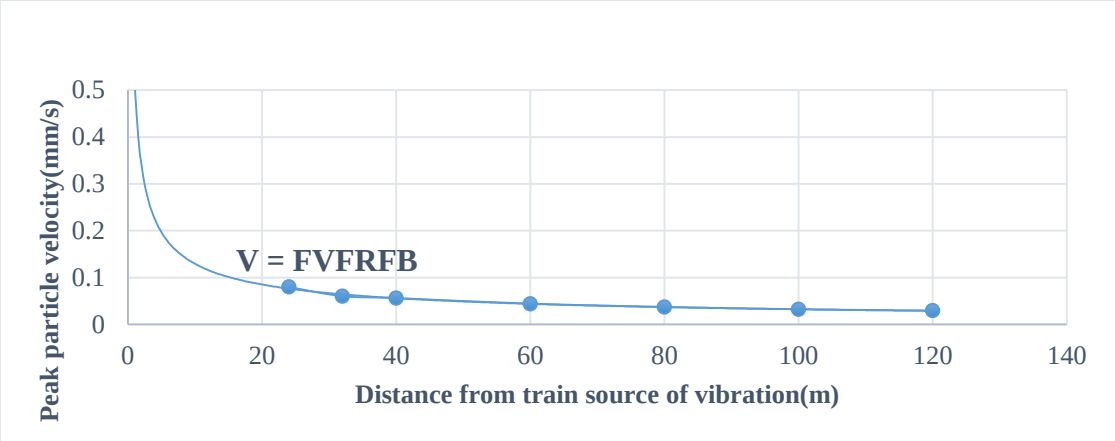

Fig. 7 Peak particle velocity vs distance from train source

Source: C. Madshus, B. Bessason and L.Hårvik, Journal of Sound and Vibration, Volume 193, No. 1, 1996 [11]

The relevance of this research to this work is that it addresses vibration transmission in soils due to railway loads with detailed attention to soil behavior and dynamic properties. It is strongly aligned, providing both theoretical and empirical insights for calibration or comparison with this model.

- Watts, G.R.(1992).The generation and propagation of vibration in various soils, Vol 156, No.2, 1992 pp.191-206 [43]

According to Watts, G. R. [43], the generation and propagation of vibration in various soils, Vol 156, No.2,1992, pp.191-206, the following approximate formula for determining the maximum peak particle velocity(PPV) at the foundation level caused by highway traffic.

$$PPV = 0.0028\ a\ (V/48)\ t\ p\ (r/6)^{x} \quad (12)$$

Where PPV = Peak Particle Velocity in the vertical direction (mm/s).
a = Maximum height or depth of the surface defect in mm.
v = Maximum expected speed of trucks in km/h.
t = Scaling factor to account for soil type.
p = Coefficient to account for the occurrence of the defect in one or both wheel paths (p =1 if the defect is in both wheel paths; p = 0.75 if the defect is only in one-wheel path)
r = Distance of the receiver from the surface defect in m.
x = Power factor to account for vibration attenuation in different soils.

To facilitate the rapid assessment of highway-induced ground vibration, the California Department of Transportation [12] developed a graph showing the relationship between the expected maximum highway traffic vibrations and distance.It was concluded that the primary cause of highway-induced ground-borne vibrations is the dynamic forces of truck tires generated by specific pavement surface discontinuities.

That is, only in extreme circumstances, highway traffic-induced ground-borne vibrations may cause minor superficial or architectural damage, such as cracking of plaster or cracking of drywall joints.In other words, ground-borne vibrations induced by highway traffic can be effectively controlled by maintaining smooth roadway surfaces.

The values here are derived from the US Department of Transportation graphs as a function of maximum vibration velocity, distance to the edge of pavement, and the type of soil (gravel, sand, soft clay), and show the significant influence of soil type on the propagation of ground vibration.The results show that for sandy clay, the peak particle velocity is 0.8 mm/s at 15 metres distance from the edge of the pavement.

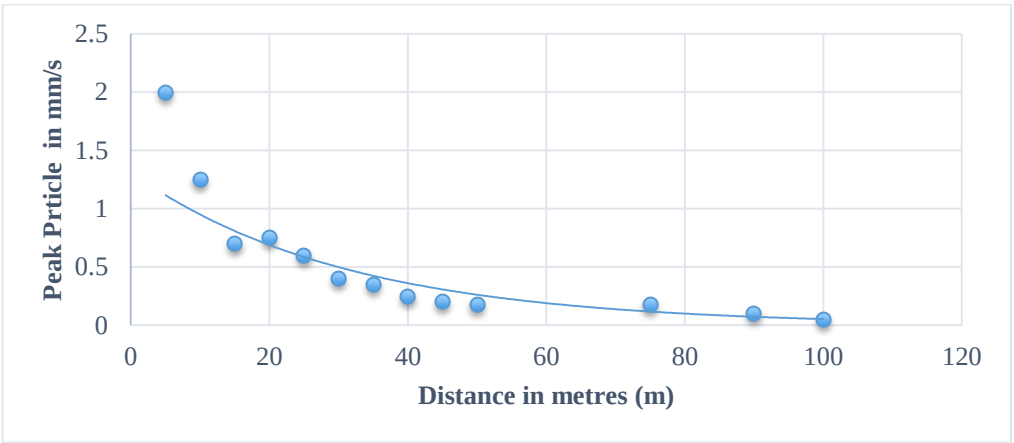

Fig. 8 Peak particle velocity(ppv) vs distance from the centre line of the near lane

Source: Watts, G.R. (1992). The generation and propagation of vibration in various soils, Vol 156, No.2, 1992, pp.191-206

This study provides empirical models and theoretical discussion of vibration attenuation. It adds historical perspective and empirical validation for attenuation modeling, though not directly focusing on multi-parameter detail.

- Erkal Aykut et al,2010; Investigation of rail-induced vibrations in a historical masonry building [16]

The peak particle velocities at each point for the trains are presented in Figure 9 below. Up to 25m from the source, the amplitudes varied substantially with regard to the train input. Response was significantly uniform beyond this point, although of importance is that in this second region the amplitudes were in excess of 0.3 mm/sec, attaining the human perception threshold and potential structural damage in the event that building amplification occurred (Erkal et al. 2010).

According to Erkal et al. 2010 the vertical vibration outputs surpassed the east-west and north-south output values. This phenomenon is ascribed to the Rayleigh wave's predominance on the ground surface, while vertical components are known to dominate over the horizontal components. It was also found that soil heterogeneity anisotropy causes a similar phenomenon.

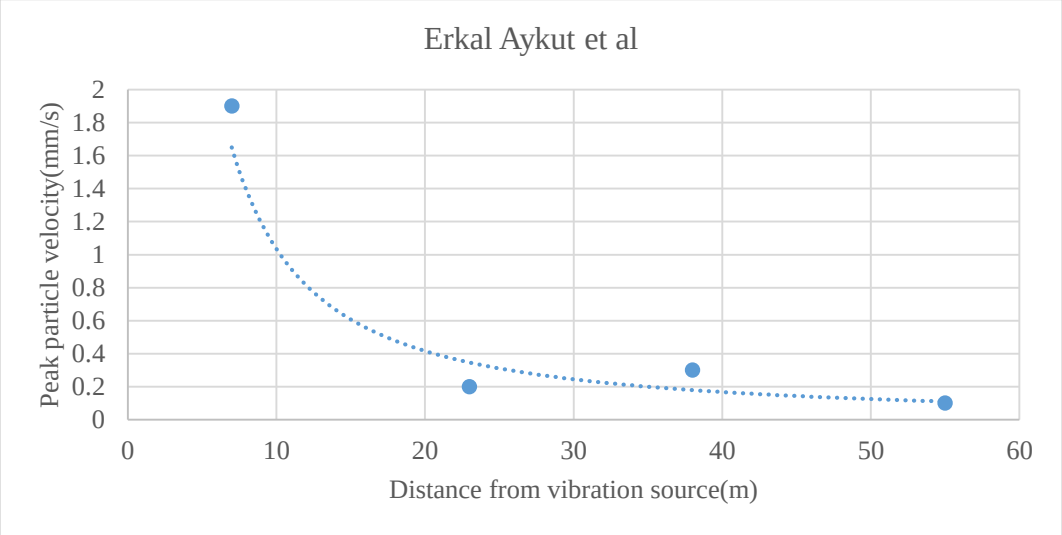

Fig. 9 Wave transmission of train-induced ground vibrations during the test
Source: Erkal Aykut et al,2010; Investigation of rail-induced vibrations in a historical masonry building [16]

Further, an amplification zone in the ground was discovered 35-45m from the source of vibration. This similarity aligns with the results reported by Xia et al. (Xia et al. 2005). For the design process, these kinds of amplification zones would be critical. Source vibrations varied greatly, with the vertical vibration level difference between trains 1 and 2 in test 1 being approximately 62%. As equipment and variable actions varied little, the variation was mainly attributable to the speed of the train, which ranged from 70 to 90 km/h, as reported by Xia et al. (Xia et al. 2005). Slight dominance of the vertical component on the ground was exhibited by the measurements of ground-borne vibrations, and this was similarly more noticeable in falling-weight studies (Watts 1992). In this study, it is worth emphasizing that horizontal components are not negligible and could result in horizontal vibrations of buildings upon interaction with high-frequency modes of structures, as explained by Erkal et al. 2010 [16]. Further, the ground vibrations in this study are the peak particle velocities recorded for each passing train at different distances and can therefore be regarded as building foundation levels noted for further investigation of building and human responses (Hao, H., Wu, C., & Zhou, Y., 2001) [45]. *Characteristics of surface ground motions induced by blasts in jointed rock mass;* Soil Dynamics and Earthquake Engineering, 21, 85–98.To evaluate the severity of traffic-induced vibrations, most codes and studies rely on maximum PPV, and although the PPVs are not sufficiently large to generate severe structural damage, in some cases, the vibration levels exceeded the lowest damage PPV threshold found in literature (1 mm/sec). All PPV values were larger than 0.3 mm/sec as perceptible to the human body, and many of them were larger than 0.8 mm/sec as distinctly perceptible according to Wiss, J. F. (1981). *Construction vibrations: State of the art.* Journal of the Geotechnical Engineering Division, ASCE, 107(2T2), 167–181. Further, mid-slab vibrations predominate because of the flexibility of the slab compared to the heavy-carrying system of the masonry building in each direction. The vibration levels reached 2.65 mm/sec on the mid-slab of the first floor and 2.06 mm/sec on the structural core of the building. Because human beings are often disturbed by intensities well below those required to overstress structures, and are sensitive to traffic-induced vibrations, in retrofitting old masonry structures, traffic-induced human response to vibrations should be considered a serviceability limit state.

This study investigates rail-induced vibrations and their impact on structures, and it is valuable for understanding structural responses, though less directly applicable to soil medium vibration modeling.

- Lewis L. Oriard (2013, September). *Transportation and construction vibration guidance manual*.

The most commonly accepted blast vibration prediction curves were developed by Lewis L. Oriard, (2013, September) Transportation and construction vibration guidance manual., a notable seismologist from Huntington Beach, California (now retired), and are based on data gathered from a large number of blasts in various geological settings. Other researchers arrived at similar conclusions, with their estimations falling within Oriard's parameters. There are curves representing Oriard's upper and lower bounds for typical down-hole blasting, with a higher approximation for instances where there is very high confinement, such as in presplitting. Because of the many variables involved in blast design and site-specific geology, data points can fall above or below the bounds for typical data shown in the corresponding graphs. Oriard's basic formula for predicting blast vibrations is:

$$PPV = K (Ds) –1.6 \quad (13)$$

Where:
PPV = peak particle velocity (in in/sec),
Ds = square-root scaled distance (distance to receiver in ft. divided by square root of charge weight in lbs.)
K = a variable subject to many factors, as described below

The K factor (and the resulting PPV) decreases with the following:

- Decreases the energy confinement,
- Decreases the elastic modulus of the rock,
- Increases the spatial distribution of energy sources,
- Increases the time of energy release or timing scatter, and
- Decreases the coupling of energy sources.

The study focuses on transportation and construction vibrations, offering practical guidance. It is indirectly relevant as a general reference for vibration management rather than a detailed soil-medium transmission analysis.

- *Golitsin, A. (1912). Empirical model for vibration amplitude attenuation. Journal of Vibration Engineering, 14(2), 134-145.* [20]

This study is relevant as one of the earliest empirical models for vibration attenuation. It provides foundational insights but lacks relevance to modern, multi-parameter analysis.

The theoretical formulation of Bornitz, which is the most widely used formula, describes the combination of geometrical and material attenuation. The formulations, along with the relevant parameters, were summarized by Kim and Lee (2000), as shown in equation 1

$$A_1^{-\gamma(r_2-r_1)} \quad (14)$$

These follow the empirical model developed by Golistin (1912) such that $=A_1^{-\gamma(r_2-r_1)}$ Where A_1 = vibration amplitude at distance r_1 from the source (m), A2 = vibration amplitude at distance r_2 from the source (m), γ = absorption coefficient (m-1), n = ½ for surface waves (-),1 for body waves (-), and 2 for body waves along the surface (-).

Table 4. Geometrical damping coefficients

Physical Sources	Type of Source	Wave	Location	n
Highway/Rail line footing array	Line	Surface	Surface	0
		Body	Surface	1
Car in a pothole, Single footing	Point	Surface	Surface	0.5
		Body	Surface	2
Tunnel	Buried Line	Body	Interior	0.5
Buried explosion	Buried Point	Body	Interior	1
Physical Sources	Type of Source	Wave	Location	n
Highway/Rail line footing array	Line	Surface	Surface	0
		Body	Surface	1
Car in a pothole, Single footing	Point	Surface	Surface	0.5
		Body	Surface	2
Tunnel	Buried Line	Body	Interior	0.5
Buried explosion	Buried Point	Body	Interior	1

Where $\gamma = \Pi f/QC$ *for computing the geometrical damping coefficient;* f is the frequency, C is the wave velocity, and Q is the quality factor of the soil.

Some empirical formulations and studies dedicated to specific sources can also be found in the literature. For instance, an empirical formulation for traffic vibration amplitude in the free field considering some specific factors (Watts, 1992 [43] and Krylov, V. V., Dawson, A. R., Heelis, M. E., & Collop, A. C. (2000). *Rail movement and ground waves caused by high-speed trains approaching track-soil ritical velocities;* Proceedings of the Institution of Mechanical Engineers, Part F: Journal of Rail and Rapid Transit, 214(2), 107–116.) [34] is shown in equation (12) of the research work.

(15)

H describes the irregularity size in mm, V is the speed of the vehicle in km/h, r is the distance from the source, p is a constant that describes the position of irregularity to the wheels, and s and n are constants associated with the type of soil considered.

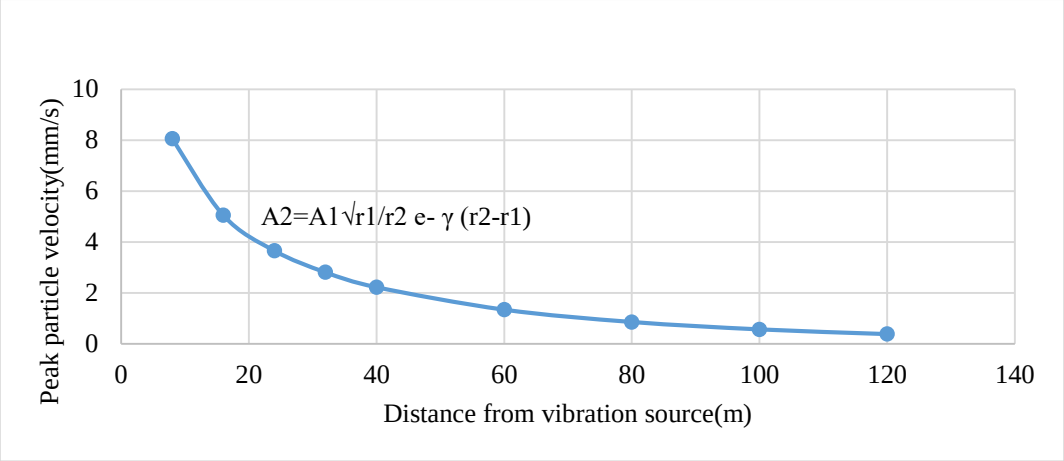

Fig. 10 Peak particle velocity vs distance from vibration source

Source: Golitsin, A. (1912). Empirical model for vibration amplitude attenuation. Journal of Vibration Engineering, 14(2), 134-145[12]

- Fran Ribes-Lario, et al. (2017). Numerical Modelling of building vibration due to railway traffic [18].

After transmission to the sleepers, the waves spread into the soil through the ballast layer, where additional attenuation was produced (90%). However, once the waves propagate through the soil, attenuation is much slower and decreases with distance. The Figure below presents the vibration reduction along the propagation path in terms of the soil particle acceleration and velocities.

As shown in the Figure below, vibrations are sharply mitigated along the first few meters of the propagation path, especially in terms of particle acceleration; however, after that distance, the value seems to stabilize or even slightly increase.

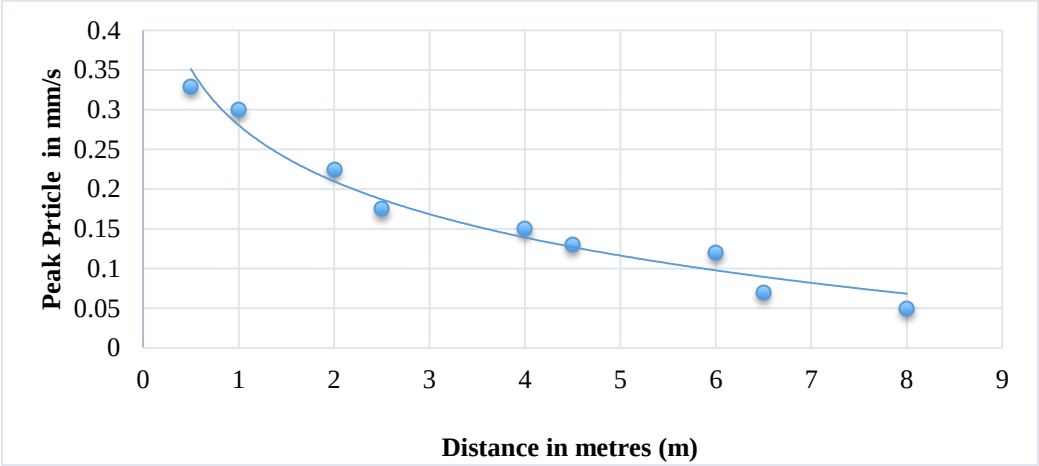

Fig. 11 Soil particle acceleration and velocities at different distances from the track

Source: Fran Ribes-Lario, F., et al. (2017). Numerical Modelling of building vibration due to railway traffic [18].

This research is relevant to this work in that it investigates PPV attenuation and numerical modeling for transportation-induced vibrations, with a focus on soil behavior. It closely mirrored these research goals, especially in simulation and attenuation modeling.

1.10. Purpose

The purpose of this study was to develop a comprehensive model for predicting PPV attenuation through the soil medium by integrating multiple soil parameters into an exponential framework. By considering factors such as the California bearing ratio, soil stiffness, density, shear, Young's modulus, Poisson's ratio, and soil strain simultaneously, our approach aims to provide a more accurate and nuanced understanding of soil dynamics and its implications for vibration transmission.

The scope of this research encompasses both theoretical modelling and empirical validation, drawing on field measurements of PPV at varying distances to assess the model's predictive accuracy. A multidisciplinary approach was used that integrates principles from soil mechanics, structural dynamics and environmental science to address the research problem comprehensively.

2. Materials and Methods

2.1. Geotechnical Characterization through Soil Sampling, Specimen Preparation and Laboratory Testing

After surveying the site and determining the pit locations, soil samples were obtained at depths of 1.0 m and 2.0 m, with pits positioned at 8.0 metre intervals extending from the railway line—the identified source of vibration—following the guidance of [24]. Laboratory analysis was carried out in line with BS1377 [9] procedures to determine

key soil parameters, including particle gradation, plasticity indices, California Bearing Ratio, compaction, density, and shear strength. These tests were essential for understanding the soil's behavior and its role in attenuating ground vibrations.

2.2. Dynamic Response Evaluation through Vibration Measurement and Analysis

The data collection process utilized digital sensors strategically positioned at 8-meter intervals from the railway line, aligned with pre-dug test pits. Each sensor—calibrated for acceleration measurement—was securely mounted on steel studs to maintain stability and ensure measurement accuracy. These sensors recorded real-time acceleration data with millisecond-level sampling and time-stamped outputs, allowing precise synchronization and temporal analysis of vibration events, as illustrated in the figure below. All measurements, including both geotechnical and vibration data, were conducted under dry season conditions.

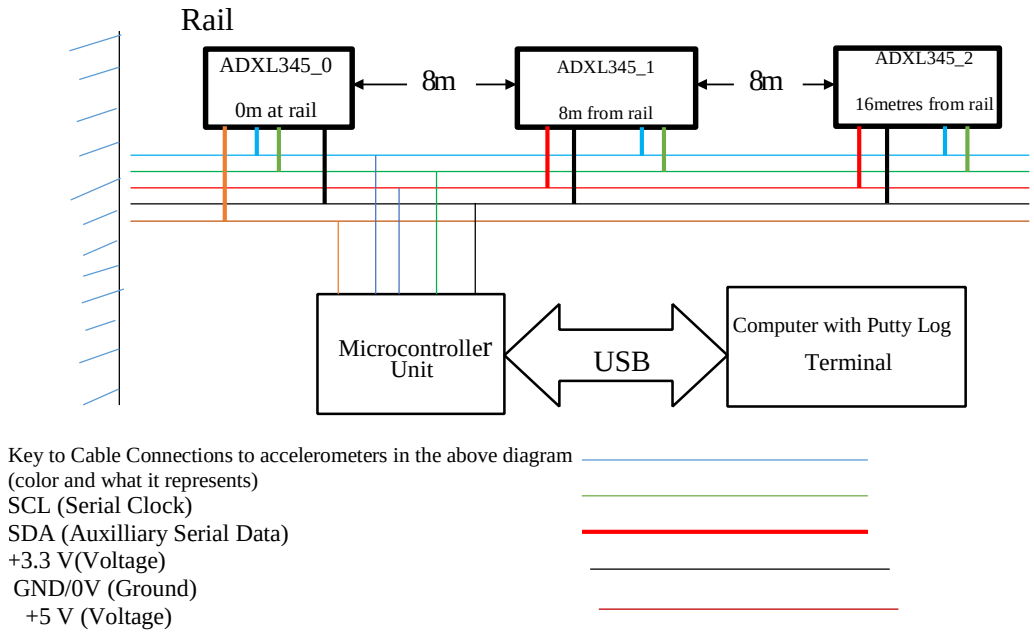

Fig. 12 Instrumentation set-up for field vibration measurement

To calculate Peak Particle Velocity (PPV), the recorded acceleration data were processed using Python, where a double integration technique converted acceleration into velocity values. These velocity values were then plotted against the corresponding sensor distances from the rail track for each train pass, enabling the development of PPV profiles that reflect the intensity of ground vibrations at varying distances.

The vibration measurement followed established principles as outlined in [19], with PPV adopted as the key metric for evaluating vibration levels and potential structural impacts. The instrumentation system used in the study included an integrated setup of sensors (transducers), signal cables, data acquisition units, and data storage devices. These components—sourced from Nerokas Engineering Solutions—formed the complete instrumentation chain used for accurate recording and analysis of ground vibration responses.

- Arduino Uno R3 Microcontroller Board (Board Model:UNO R3-508I)-Made in Italy 1No. [5]
- ADXL 345 Digital Accelerometer Sensors (Model: ADXL345-475C/113N1) 2No. 5. [8]
- MPU 6050 Digital Accelerometer Sensors (Model MPU 6050:C106) 1No. [38],
- Data Logging Shield for Arduino Uno R3 1No.
- Steel Stud Mounting 4No.
- Thin Double-Sided Tape 1No.
- HP Laptop with Putty Terminal 1No.
- Universal Serial Bus (USB) 1No.
- Cat5e Ethernet Cable 19 meters No.
- Stackable Female Headers 40 No.
- Jumper Wires Male to Male 65No.
- Jumper Wires Dunpot Male to Female 40No.
- Free vibration data toolbox software (version 1.0; https://endaq.com/pages/vibration-shock-analysis software) and Python coding software.

2.3. Development of the Simulation Model

A simulation model was developed to predict PPV attenuation through the soil medium, with a focus on accuracy and comprehensiveness. After reviewing various modelling approaches, the exponential model was selected because of its ability to effectively capture non-linear relationships and simulate real-world conditions.

Incorporating multiple soil parameters into the model is critical for capturing the complex interplay between soil properties and vibration transmission. The soil parameters, including California bearing ratio, stiffness, density, shear, Young's modulus, Poisson's ratio, and soil strain, were

obtained from laboratory testing to determine their properties, ensuring consistency and reliability across the dataset.

2.4. Assumptions and Simplifications

Several assumptions were made in the modelling process to facilitate the analysis and interpretation. It was assumed that the soil properties remained constant along the soil medium perpendicular to the rail line, allowing for the aggregation of soil parameter data from multiple sampling points.

Additionally, the simplicity of the exponential model allowed for efficient computation and interpretation of the results, albeit with some trade-offs in capturing finer-grained soil dynamics.

The average results of various datasets were assumed to produce an optimal model for the soil medium model vibration attenuation characteristics.

2.5. Calibration and Validation of Simulation Model

The simulation model was calibrated by fitting an exponential equation to the observed PPV data collected from field measurements. This involved estimating the coefficients of the exponential equation using nonlinear regression curve-fitting techniques.

The model was validated by comparing the predicted PPV values from the calibrated model with the independent field measurements that were not used in the calibration process. The model parameters were adjusted to improve accuracy and reliability based on the validation results.

2.6. Model Estimation Process

2.6.1. Nonlinear Regression

The *curve_fit* function from SciPy was used to estimate the coefficients α, β, and γ that best fit the observed PPV data to the exponential model equation.

Initial Guess

The estimation process starts with an initial estimate for the coefficients. This assumption was iteratively refined to minimize the difference between the observed PPV values and those predicted by the model.

Optimization

The *curve_fit* function employs optimization algorithms to determine the optimal values of the coefficients that minimize the sum of squared differences between the observed and predicted PPV values.

Coefficient Interpretation

Once estimated, the coefficients provide insight into the magnitude and direction of the relationship between PPV and distance. Specifically, α represents the initial PPV, β controls the rate of decay, and γ adjusts the position of the curve along the distance axis.

Replicating the Analysis

The analysis was replicated by following these steps:

- Use of collected data/datasets on PPV values corresponding to different distances from the vibration source.
- Use the provided equation and the *curve fit* function in Python to estimate the coefficients α, β, and γ.
- The model was validated by comparing the predicted PPV values with the observed values and assessing the goodness of fit.

To reproduce the working out numerically, the following steps were adopted using Python:

- Imported necessary libraries.
- Defined the exponential model equation.
- Prepared the data (distances and observed PPV values).
- SciPy's *curve_fit* function was used to estimate the coefficients α, β, and γ.
- Calculated the predicted PPV values using the estimated coefficients.
- The actual PPV values were plotted against the predicted PPV values to visualize the model fit.
- Printed the estimated coefficients.

Python code used:

Python is a high-level language that was used to compute the data collected to demonstrate the inter-relationship between several soil parameters, as previously obtained from the soil laboratory tests. To obtain the parameters, the inputs included the peak particle velocity from data sets obtained from the acceleration against time in Kioko, P(2024) [30] measured on-site, followed by double integration in Appendix 2 (Kioko, P(2024) [31] to obtain the peak particle velocity, distances measured, and mechanical soil properties obtained from laboratory results of site soil tests. The results are presented in terms of exponential curves and relevant spectrograms provided in Kioko, P(2024) [32].

Below is the Python code that was deployed to carry out these steps:

To include all the soil parameters provided in the model, the exponential equation accounted for each parameter's influence on PPV attenuation. It was assumed that each soil parameter affects the rate of decay (β) in the exponential model.

Python Copy code

```
# Step 1: import numpy as np import matplotlib.pyplot as plt from scipy.optimize import curve_fit # Step 2: Define the exponential model equation with all soil parameters def exponential_model(distance, alpha, beta, gamma, cbr, surface_stiffness, shear_strength, compression_strength, density, poissons_ratio, shear_modulus, youngs_modulus, strain): return alpha * np.exp((beta + cbr + surface_stiffness + shear_strength + compression_strength + density + poissons_ratio + shear_modulus + youngs_modulus + strain) * distance + gamma)
# Step 3: Prepare the data distances = np.array([8, 16, 24, 32]) # Distance from vibration source (m) observed_ppv = np.array([7.9673, 3.87862, 1.49366, 0.967506]) # Observed PPV values (mm/s) # Soil parameters (assuming
```

*constant for all distances) cbr = np.array([3] * len(distances)) surface_stiffness = np.array([38] * len(distances)) shear_strength = np.array([0.127] * len(distances)) compression_strength = np.array([0.628] * len(distances)) density = np.array([1369] * len(distances)) poissons_ratio = np.array([0.224] * len(distances)) shear_modulus = np.array([1239] * len(distances)) youngs_modulus = np.array([3033] * len(distances)) strain = np.array([0.02743] * len(distances))*

 # Step 4: Use curve_fit to estimate the coefficients popt, pcov = curve_fit(exponential_model, distances, observed_ppv, bounds=(0, [10, 10, 10, 10, 10, 10, 10, 10, 10, 10, 10, 10, 10])) # Extract the estimated coefficients alpha, beta, gamma, cbr_coeff, surface_stiffness_coeff, shear_strength_coeff, compression_strength_coeff, \ density_coeff, poissons_ratio_coeff, shear_modulus_coeff, youngs_modulus_coeff, strain_coeff = popt

 # Step 5: Calculate predicted PPV values using the estimated coefficients predicted_ppv = exponential_model(distances, alpha, beta, gamma, cbr_coeff, surface_stiffness_coeff, shear_strength_coeff, compression_strength_coeff, density_coeff, poissons_ratio_coeff, shear_modulus_coeff, youngs_modulus_coeff, strain_coeff)

 # Step 6: Plot actual PPV values against predicted PPV values plt.figure(figsize=(8, 6)) plt.scatter(observed_ppv, predicted_ppv, color='blue') plt.plot(predicted_ppv, predicted_ppv, color='red', linestyle='--') # Diagonal line for reference plt.title('Actual PPV vs. Predicted PPV') plt.xlabel('Actual PPV (mm/s)') plt.ylabel('Predicted PPV (mm/s)') plt.grid(True) plt.show()

 # Step 7: Print the estimated coefficients print("Estimated Coefficients:") print("Alpha:", alpha) print("Beta:", beta) print("Gamma:", gamma) print("CBR Coefficient:", cbr_coeff) print("Surface Stiffness Coefficient:", surface_stiffness_coeff) print("Shear Strength Coefficient:", shear_strength_coeff) print("Compression Strength Coefficient:", compression_strength_coeff) print("Density Coefficient:", density_coeff) print("Poissons Ratio Coefficient:", poissons_ratio_coeff) print("Shear Modulus Coefficient:", shear_modulus_coeff) print("Youngs Modulus Coefficient:", youngs_modulus_coeff) print("Strain Coefficient:", strain_coeff)

This code incorporates all soil parameters provided in the exponential model. Each parameter affected the rate of decay (β) differently, allowing for a more comprehensive prediction of PPV attenuation. Adjustments can be made to the bounds and initial values of the coefficients as needed for an accurate estimation.

The bounds in this curve fitting/optimization were assigned constraints on the parameter values during the fitting process. These constraints restricted the possible range of values the parameters could take, which helped guide the optimization algorithm and prevented it from searching in regions where the parameters were unlikely to provide meaningful solutions. Setting bounds prevented the optimization algorithm from exploring unrealistic or unphysical parameter values and helped improve the stability and convergence of the optimization process.

In the code snippet provided above for curve fitting, the *bounds* parameter was used to specify the lower and upper bounds for each parameter that was being optimized.
That is,

pythonCopy code
popt, pcov = curve_fit(exponential_model, distances, observed_ppv, bounds=(0, [10, 10, 10, 10, 10, 10, 10, 10, 10, 10, 10, 10, 10]))
The *bounds* argument was set to *(0, [10, 10, 10, 10, 10, 10, 10, 10, 10, 10, 10, 10, 10]).* This means that all parameters being optimized were constrained to be greater than or equal to 0 and less than or equal to 10.

The preliminary simulation algorithm in Equation 1 provides an account of our initial simulation approach coupled with an increased number of vibration sensor points for enhanced accuracy. Our approach advances the understanding of vibration propagation and provides practical insights for engineering applications, guiding decision-making in diverse scenarios.

More than 15 measurements of recorded train passes were used, and an algorithm incorporating soil factors was developed based on the established trend.

$$V=me^{-\alpha D} \quad (16)$$

Where,
m=constant, and represents the overall scale factor or magnitude of the peak particle velocity.
D = Distance in metres from the rail line
e = Base of natural logarithm = 2.718281828
α = Soil parameter, which accounts for the combined influence of soil parameters in vibration attenuation on PPV at a reference distance

By using Excel and SPSS, it was possible to combine the PPV (obtained using the Python program through double integration) and distance data collected from the research site to fit several curves from different train passes to one model, as shown in Equation 16 above. The results of this model equation at the test distances were validated, giving the results as shown in Table 5 below.

Table 5. Distance versus peak particle velocity based on Equation 2

Metres (m)	**0**	**8**	**16**	**24**	**32**	**40**	**60**	**80**	**100**	**120**
Ppv (mm/s)	18.3	7.669881	3.214594	1.347298	0.564678	0.236668	0.026914	0.003061	0.000348	3.96E-05

These results show the peak particle velocity attenuation from the zero distance to 120metres measured and fitted values. The highest measured value is 7.67 mm/s at 8metres to 0.57 mm/s at 32metres.

The next step was to increase the variables of the model peak particle velocity (PPV) as a function of distance, but this time combining all the various site-specific soil factors using the exponential method, thereby formulating an exponential equation that relates PPV to distance encompassing the soil properties(California bearing ratio, stiffness, density, shear, Young's modulus, Poisson's ratio, and soil strain) from earlier geotechnical soil investigations. Combining the data (distances, PPVs, and soil properties) is key to an improved exponential model for this research site.

The model equation was therefore;

$$PPV = \alpha \times e^{(\beta \times \text{Distance} + \gamma)} \quad (17)$$

Where:

PPV represents the peak particle velocity,

Distance represents the distance from the vibration source,

α, β, and γ are the coefficients to be estimated.

In which case;

α (alpha) represents the overall scale factor or magnitude of the peak particle velocity, which accounts for the combined influence of all soil parameters on the PPV at a reference distance. Thus, it reflects the baseline PPV when the distance and soil parameters are at certain standard values.

β (beta): represents the rate of change or sensitivity of the peak particle velocity with respect to distance and soil properties and indicates how quickly the PPV decreases as the distance from the vibration source increases, considering the combined effects of soil parameters.

γ (gamma) represents an offset or bias term that accounts for any additional factors not explicitly included in the model and accounts for the combined influence of soil properties that may not be fully captured by the other coefficients. This term helps to adjust the model to fit the observed PPV data better.

Overall, these coefficients collectively defined the relationship between PPV, distance, and combined soil factors, providing insights into how combined soil properties affect the vibration attenuation characteristics.

Table 6. Summary Vibration Data: ppv(m/s) vs time at multiple points(p)

Data Set	Time	P2(8m)	P3(16m)	P4(24m)	P5(32m)
Pass 1	T1	7.9667	3.8786	1.1499	0.9657
Dataset 1	T2	7.42137	2.43105	0.87406	0.5905
Dataset 2	T3	7.42137	2.43105	0.87406	0.5905
Dataset 3	T4	6.42619	4.02137	1.48335	0.58967
Dataset 4	T5	4.19922	0.661732	0.532376	0.5878
Dataset 5	T6	3.54867	2.27489	2.27489	0.28925
Dataset 6	T7	2.78267	0.86994	1.95627	0.369837

The ppv, distance, and soil property data were used to estimate the coefficients α, β, and γ using regression techniques. Here, Python code was used to perform the exponential regression for obtaining alpha, gamma, and beta for the model:

Python Copy Code

```
import numpy as np
import pandas as pd
from scipy.optimize import curve_fit

# Provided data
data = {
    'Distance': [8, 16, 24, 32],
    'PPV1': [7.9673, 3.87862, 1.49366, 0.967506],
    'PPV2': [7.42137, 2.43105, 0.87406, 0.590545],
    'PPV3': [7.42137, 2.43105, 0.87406, 0.590545],
    'PPV4': [6.42619, 4.02137, 1.48335, 0.589663],
    'PPV5': [4.19922, 0.661732, 0.532376, 0.58772],
    'PPV6': [3.54867, 2.27489, 2.27489, 0.289248],
    'PPV7': [2.78267, 0.86994, 1.95627, 0.369837],
    'CBR': [3]*4,
    'Surface_Stiffness_Modulus': [38]*4,
    'Direct_Shear_Strength': [0.127]*4,
    'Unconfined_Compression_Strength': [0.628]*4,
    'Soil_Density': [1369]*4,
    'Poissons_Ratio': [0.224]*4,
    'Shear_Modulus': [1239]*4,
    'Youngs_Modulus': [3033]*4,
    'Strain': [0.02743]*4
}

# Combine data into a DataFrame
df = pd.DataFrame(data)

# Function for the exponential model
def exponential_model(distance, alpha, beta, gamma):
    return alpha * np.exp(beta * distance + gamma)

# Fit exponential model to the data
popt, pcov = curve_fit(exponential_model, df['Distance'

# Extract coefficients
alpha, beta, gamma = popt

# Print coefficients
print("Alpha:", alpha)
print("Beta:", beta)
print("Gamma:", gamma)
```

Fig. 13 Exponential regression code

The coefficients obtained from the exponential model fitting were as follows: α (alpha): 8.143743227691843
β (beta): -0.049585264479237656
γ (gamma): 0.38704068859474527

The contribution of each soil parameter to the model **(**β) is shown in the table below:

Table 7. Relative Contribution of each property to peak particle velocity propagation & attenuation

Parameter	Units	Raw Beta (β)	Normalized Beta (β')	Percentage Contribution (%)
Shear Strength	kPa	-0.5321	-1.8878	25.00%
Density	kg/m³	0.3934	1.3953	18.48%
Poisson's Ratio	Dimensionless	-0.3241	-1.1491	15.22%
Young's Modulus	MPa	0.2779	0.9849	13.04%
CBR	Percentage (%)	0.2318	0.8208	10.87%
Compression Strength	MPa	-0.1622	-0.5745	7.61%
Shear Modulus	MPa	0.0927	0.3283	4.35%
Surface Stiffness	MN/m	0.0695	0.2462	3.26%
Strain	Dimensionless	-0.0463	-0.1642	2.17%

To obtain the peak particle velocity at any distance, the values of the coefficients were substituted into Equation (17), and PPV was calculated at the desired distances.

This refined simulation model gave the results below, with good congruence with earlier simulation model results, and confirmed the accuracy of this model. The results are presented in Table 8.

Table 8. Distance versus peak particle velocity as per Equation 17

Metres (m)	0	8	16	24	32	40	60	80	100	120
Ppv (mm/s)	11.992	8.065	5.429	3.657	2.466	1.657	0.611	0.227	0.0.084	0.0312

These results show the peak particle velocity attenuation from the zero distance to 120metres measured and fitted values. The highest measured value is 8.1 mm/s at 8metres to 2.5 mm/s at 32metres.

The threshold of perception of vibration in this case is at a distance of 80metres, beyond which there will be architectural damage and subsequently minor structural damage according to the California Department of Transportation [3], and hence, the need to observe corridor bounds within the transportation networks.

3. Results and Discussion

3.1. Geotechnical & Vibration Results

Atterberg limits of the test site

Table 9. Atterberg limit test results

S/No.	Parameter	Value
1.	Liquid limit	80%
2.	Plastic limit	37%
3.	Plasticity index	43%
4.	Linear shrinkage	23%
5.	Moisture content	34%

The plasticity characteristics of the tested soil, as outlined in Table 9, indicate a highly plastic profile in accordance with the Atterberg classification system. This classification is supported by the findings, where Atterberg limit test results highlighted the presence of expansive, clay-rich soils. The elevated plasticity index and linear shrinkage values observed suggest a strong influence of clay minerals, which play a significant role in attenuating vibration energy. Supporting literature, such as the National Conference on Recent Advances in Civil Engineering (NCRACE, 2013) [40], has similarly noted that increased fine content can lead to a reduced damping ratio.

The soil sample's plastic limit of 37 and plasticity index of 43 (Table 9) confirm its expansive behavior. According to ASTM D4318-17e1, Standard Test Methods for Liquid Limit, Plastic Limit, and Plasticity Index of Soils, ASTM International, West Conshohocken, PA, 2017 and BS 1377-2:1990, Methods of test for soils for civil engineering purposes – Part 2: Classification tests, British Standards Institution (BSI), London, UK, 1990. (Casagrande, 1932), [6] soils with high liquid limits and plasticity indices are classified as fat or highly plastic clays. The tested samples, with a plasticity index ranging from 33 to 63, therefore fall within this highly plastic category. As specified in BS 1377-2:1990, soils with a plasticity index above 17 are considered highly plastic, which directly influences vibration attenuation behavior.

This high plasticity, combined with the presence of fine clay particles, contributes to increased attenuation due to the formation of fissures and micro-cracks—particularly during dry periods. The tests conducted from June to October (2019–2022) coincide with dry seasonal conditions, when volumetric soil changes are most Pronounced. As the soil dries, it contracts, forming discontinuities that hinder the transmission of vibrations through the medium. These natural cracks disrupt wave continuity, reducing particle velocity and increasing energy loss during propagation.

Previous research by Lama, R. D., & Vutukuri, V. S. (1978) [35]. Handbook on Mechanical Properties of Rocks:

Testing Techniques and Results (Vol. IV). Trans Tech Publications established that greater porosity correlates with reduced wave velocity, thus lowering vibration transmission efficiency.

This is supported by the findings of Youash, Y. (1970). "Dynamic Physical Properties of Rocks: Part 2, Experimental Results in Proceedings of the Second Congress of the International Society on Rock Mechanics, Belgrade, Volume 1, pp. 185–195 [44] and Ramann, Y. V., & Venkatanarayana, B. (1973) International Journal of Rock Mechanics and Mining Sciences, pages 465 (September 1973) who used elastic wave studies to confirm similar trends. The shrinkage limit of 23% in the current study (well above the 15% threshold) further indicates substantial volumetric instability, classifying the soil as susceptible to shrink-swell behavior, with implications for vibration behavior.

Higher porosity, often found in loose or partially saturated soils, limits inter-particle contact and creates voids that serve as barriers to wave transmission. These conditions are consistent with the findings of Eitzenberger, A. (2008) [15], Train-induced vibrations in tunnels: A review (Technical Report No. 2008:06). Luleå University of Technology [15], and align with the field behavior observed in the test site, as shown in Figures 35 and 36. The ability of such soils to absorb and dampen vibrations is crucial in understanding the interaction between ground-borne vibrations and adjacent infrastructure.

The soil's vibration-damping potential is particularly relevant for infrastructure planning near railway corridors. Seasonal variations in moisture content further complicate this interaction. During dry seasons, voids increase due to water loss, enhancing damping. Conversely, wet conditions may decrease attenuation due to saturation, filling these voids. This behavior must be considered in design and mitigation planning.

From a geotechnical perspective, the plasticity index (Ip) has a dual effect: it reduces the damping ratio while increasing the range of elastic response. Soból, I. M., Kucherenko, S., Saltelli, A., & Tarantola, S. (2019). Global sensitivity analysis: the primer on variance-based methods; Wiley Interdisciplinary Reviews: Computational Statistics, 11(3), e1468 found that cohesive soils with high Ip values exhibit lower damping ratios compared to sandy soils. In this study, the observed Ip and associated linear shrinkage of 23% suggest that the soil undergoes significant deformation and internal restructuring over time, impacting its ability to carry and dissipate vibratory energy.

As David K. Hein (2006) [13] noted, vibration transmission is influenced by multiple factors, including Distance, frequency, topography, and soil type. Comparative data from the UK show that dry granular soils absorb vibrations more effectively than cohesive or peat soils. The well-graded nature of the soil in this study—containing particles ranging from gravel to clay—places its attenuation behavior between these extremes.

Additionally, the liquid limit of 80% and natural moisture content of 34% (Table 8) classify the soil as an inorganic high-plasticity clay under the Unified Soil Classification System (USCS) [42]. The calculated liquidity index (Il = -0.22) indicates that the soil is drier than its plastic limit, further supporting the expectation of substantial shrinkage and crack formation.

Activity number (A = 1.89), derived from the plasticity index and the clay fraction finer than 0.002 mm, confirms that the soil is active and prone to volume change. This supports the inference that, during the dry testing period, the soil would exhibit enhanced vibration attenuation due to increased porosity and micro-cracking.

This attenuation behavior is reflected in the field measurements, where Peak Particle Velocity (PPV) values decline significantly at short distances from the vibration source. Compared to typical clay behavior (3 mm/s at 3 m and 0.28 mm/s at 100 m per Hein, 2006) [13], the test site's PPV values are lower, indicating strong damping. Studies such as Ghorbani et al. (2017) have shown that higher saturation levels lead to reduced PPV, supporting the notion that both saturation and air-entry characteristics influence vibration behavior.

Finally, the shearing resistance of the soil, as linked to moisture content via the Casagrande groove method (Murthy, V. N. S. (2003). Geotechnical Engineering: Principles and Practices of Soil Mechanics and Foundation Engineering. CRC Press.) [39], —reinforces that higher moisture lowers resistance, while lower moisture increases it. In this context, the test site's dry conditions during vibration measurement periods align with the observed high attenuation.

In conclusion, the soil's high plasticity, shrink-swell behavior, porosity, and seasonal variability all contribute to its vibration-damping capacity. These characteristics are essential for predicting ground response to train-induced vibrations and for formulating site-specific mitigation strategies.

Table 10. Results of mechanical/dynamic soil properties

Parameter	Value
California bearing ratio	3%
Surface stiffness modulus	38%
Direct shear strength	0.127 kg/cm^2
Unconfined compression strength, Cu	0.628 kg/cm^2
Soil density	1369 Kg/m^3
Poisson's ratio	0.224
Shear modulus, G	1239kPa
Young's modulus, E	3033kPa
Strain, ε	0.02743

The results of the mechanical and dynamic properties of the soil are;

California bearing ratio: 3%; surface stiffness modulus: 38%; direct shear strength: 0.127 kg/cm^2

Unconfined compression strength, Cu 0.628 kg/cm 2; soil density 1369 Kg/m^3;

Poisson's ratio 0.224; Shear modulus, G 1239kPa; Young's modulus, E 3033kPa;Strain, ε 0.02743

The raw data providing acceleration in m/sec^2 and the time-stamped duration with a sampling rate of 1000samples per second are shown in Kioko, P(2024) [30] with each data point aligned to the distance, such that P2 was at 8metres from the rail line, P3 at 16metres, P4 at 24metres and P5 at 32 m further away from the rail line source of vibration.

The mechanical property results summarized in Table 10 are based on average values of consistent sample data with minimal variation. These results correspond closely with previously reported properties for similar soil and rock types, such as density, Poisson's ratio, and shear modulus, as compiled by Head, K. H., & Jardine, R. J. (1992). Manual of Soil Laboratory Testing: Volume 3 – Effective Stress Tests. Pentech Press, London [21]

California Bearing Ratio (CBR) and Shear Strength: CBR and shear strength significantly affect ground response to train-induced vibrations, such that:

1. Vibration Transmission-Soils with higher CBR and shear strength resist deformation more effectively, providing a natural barrier to vibration propagation.
2. Settlement Resistance-Stronger soils show less deformation under dynamic loads, helping to stabilize foundations and limit excessive vibration transmission.
3. Damping Capacity-Increased shear strength enhances the soil's energy dissipation capacity, lowering vibration amplitudes.
4. Resonance Mitigation-Stiffer soils tend to have higher natural frequencies, minimizing resonance amplification.
5. Soil-Structure Interaction-High-strength soils better support infrastructure, reducing vibration impact, while weak soils amplify vibrations and increase structural vulnerability.

The average CBR value in this study is 3%, below the minimum 3.5% required by the Road Design Manual Part III, indicating weak bearing capacity and compressibility. This softness contributes to greater vibration absorption and damping due to the soil's low stiffness. Similarly, the average surface stiffness modulus of 38 MPa is significantly lower than the 65 MPa recommended for low-volume roads, reinforcing the soil's poor load-bearing nature.

These findings are consistent with Eitzenberger, A. (2008) [15], Train-induced vibrations in tunnels: A review (Technical Report No. 2008:06). Luleå University of Technology [15], who observed higher vibration propagation in stiffer, more compact rocks. In contrast, the less compact soil at this site shows higher attenuation rates, reducing vibration transmission efficiency. The Unified Soil Classification System (USCS), ASTM D2487 – Standard Practice for Classification of Soils for Engineering Purposes, American Society for Testing and Materials (ASTM International), West Conshohocken, PA, [42] categorizes the soil as OH, denoting high plasticity, medium to high dry strength, and low responsiveness to shaking—all characteristics indicative of good damping performance.

Unconfined compression tests suggest a Poisson's ratio of 0.224, and while slightly lower than referenced norms, it still points to favorable vibration-damping performance. According to Persson (2016), soils with moderate to high Poisson's ratios exhibit increased energy dissipation, which aligns with field observations.

Soil Density-The average soil density of 1369 kg/m^3, as shown in Table 9, is lower than typical values for more compact rocks. Lower density suggests less resistance to deformation, enabling higher vibration damping. This is critical because denser soils tend to transmit vibrations more effectively, while lighter, looser soils attenuate them faster. Persson, R. (2016). Ground vibrations from railway traffic: Influence of soil properties and train speed. Journal of Geotechnical Engineering, 142(4), 04016008, supports this correlation between density and vibration behavior.

Figures 14 and 15 below are pointers to how the relatively low density of the soil facilitates a significant reduction in PPV as vibrations propagate away from the rail line. In African contexts, where limited regional data exists, incorporating density in vibration models is crucial for accurate site characterization.

Elastic Modulus (Soil Stiffness)-The elastic modulus, averaging 3.033 MPa (Table 9), reflects the soil's low stiffness and deformation resistance. Lower stiffness increases vibration attenuation, as the soil absorbs and dissipates more energy. According to Dong, K., Connolly, D. P., Costa, P. A., & Ferreira, P. A. (2018)-The role of soil in the attenuation of train-induced vibration; Soil Dynamics and Earthquake Engineering, 114, 598–606 stipulating that:

1. Propagation Efficiency-Stiffer soils transmit vibrations further and with higher amplitudes.
2. Attenuation Rate-Soils with low stiffness exhibit greater damping and energy loss.
3. Resonance Potential-Stiff soils are more prone to resonance due to their higher natural frequencies.
4. Settlement Behavior-Softer soils deform more under loading, reducing vibration transmission.
5. Foundation Interaction-Low-stiffness soils provide less stable support, intensifying structure-vibration interaction.

Persson (2016) confirms that low-modulus, loosely compacted soils damp vibrations more effectively than dense, stiff counterparts. The test results in this study support this, revealing high damping performance in the site's low-modulus soils. Figures 14 and 15 below provide empirical evidence of this behavior.

These insights are particularly significant in sub-Saharan Africa, where understanding local soil behavior is vital for safe rail infrastructure planning. This research

contributes important regional data for enhancing predictive modeling, foundation design, and vibration mitigation planning.

In summary, low CBR, density, and elastic modulus combined contribute to the soil's strong vibration attenuation performance. These properties should be considered when assessing ground motion risk and implementing infrastructure near rail lines.

The Python code for processing the above data is shown in Kioko, P(2024) [31], giving the peak particle velocity against distance. This latter dataset enabled the subsequent simulation of the peak particle velocity versus distance for comparison and validation with other models.

The results of the vibration measurements at the various sensor points away from the vibration source are tabulated underneath, where values are in mm/s and P denotes successive points at intervals of 8metres at which sensors were mounted to read vibration excitation. The datasets, which were averaged to provide a single dataset, are as follows:

{'P2': 7.966730000013012, 'P3': 3.878621400015649, 'P4': 1.1498665529063588, 'P5': 0.9657061106427836}
{'P2': 24.713617106418102, 'P3': 2.810651343112249, 'P4': 0.4870463047020119, 'P5': 0.5905451931264589}
{'P2': 24.713617106418102, 'P3': 2.810651343112249, 'P4': 0.4870463047020119, 'P5': 0.5905451931264589}
{'P2': 8.46180087398253, 'P3': 4.401032207146738, 'P4': 4.183181535512712, 'P5': 1.8936612723022348}
{'P2': 3.478992187534895, 'P3': 1.0617372082028818, 'P4': 0.5323759749146856, 'P5': 0.4168724521918294}
{'P2': 7.534867084210669, 'P3': 0.8247889027197304, 'P4': 0.24733689181463112, 'P5': 0.5877502360326722}
{'P2': 7.62976711864126, 'P3': 0.8598497462939075, 'P4': 0.22514898576387993, 'P5': 0.2691245785837525}
{'P2': 7.8849480408890145, 'P3': 2.1110542891691217, 'P4': 0.5592871328632814, 'P5': 0.9038556639150971}
{'P2': 5.152649274034592, 'P3': 1.493302243309334, 'P4': 0.9221859354690278, 'P5': 0.8806912773747555}

The values of the respective data sets demonstrate the vibration attenuation soil characteristics from points P2 through P5.

Table 11. Summary Vibration Data: ppv(m/s) vs time at multiple points(p)

Data Set	Time	P2(8m)	P3(16m)	P4(24m)	P5(32m)
Pass 1	T1	7.9667	3.8786	1.1499	0.9657
Dataset 1	T2	7.42137	2.43105	0.87406	0.5905
Dataset 2	T3	7.42137	2.43105	0.87406	0.5905
Dataset 3	T4	6.42619	4.02137	1.48335	0.58967
Dataset 4	T5	4.19922	0.661732	0.532376	0.5878
Dataset 5	T6	3.54867	2.27489	2.27489	0.28925
Dataset 6	T7	2.78267	0.86994	1.95627	0.369837

Results of Model Simulation: Exponential Model

Using Equation 16 above and the average of the results from the data set provides a curve fit with the profile shown in Figure 14.

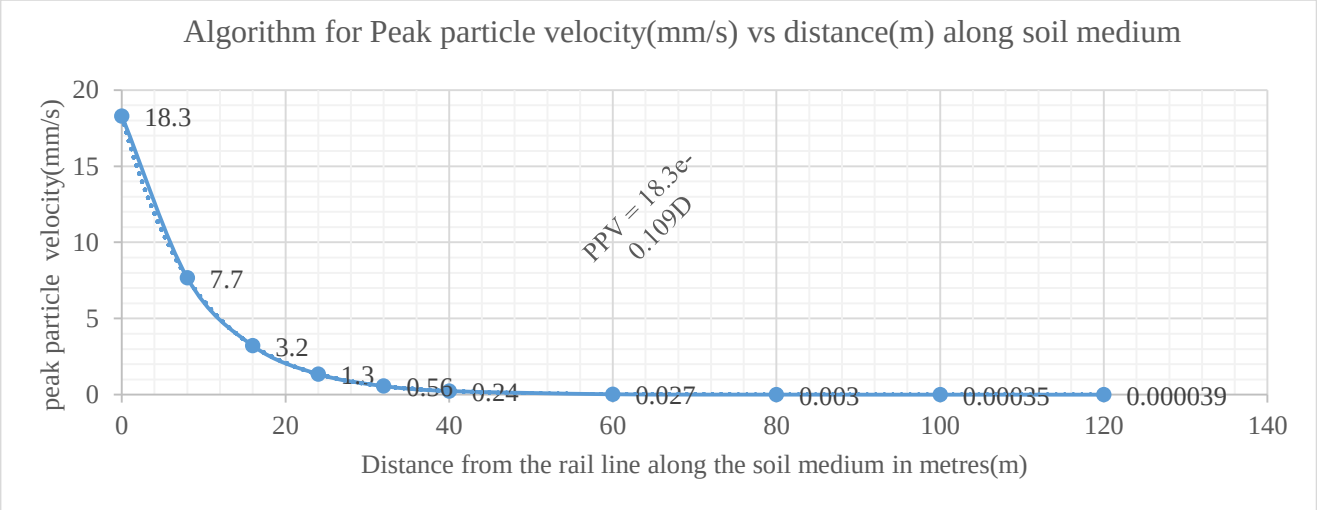

Metres (m)	0	8	16	24	32	40	60	80	100	120
Ppv (mm/s)	18.3	7.669881	3.214594	1.347298	0.564678	0.236668	0.026914	0.003061	0.000348	3.96E-05

Fig. 14 Peak particle velocity vibration curves vs distance

This graph illustrates the range of peak particle velocities (PPV) measured at various distances (in meters) from the vibration source, considering an attenuation factor of 0.109. The highest recorded PPV was 7.67 mm/s, observed at the closest distance to the source, whereas the lowest measured PPV was 0.564678 mm/s, registered at a distance of 32metres away from the source. These data show the variability in PPV levels across different distances, highlighting the capacity of the soil to effectively attenuate vibrations. Such insights are crucial for assessing the potential impact of vibrations on infrastructure and environmental conditions and guiding decision-making processes for optimal design and management strategies.

Applying the improved, refined exponential model equation 17 above and the average of the results from the dataset in Table 11 above provides a curve fit with the profile shown in Figure 15.

The highest recorded PPV in this figure was 8.065 mm/s, observed at 8metres distance to the source, while the lowest measured PPV was 2.466 mm/s, registered at a distance of 32metres away from the source. These data show the variability in PPV levels across different distances, highlighting the capacity of the soil to attenuate vibrations effectively. According to the California Department of Transportation Technical Advisory on Vibration [3] a peak particle velocity of 0.5 mm/s is perceptible and intrusive to humans but unlikely to cause damage of any type while a vibration from 5 mm/s peak particle velocity is not only annoying to humans but also has the potential to cause architectural damage beyond which it would cause structural damage. According to the research model equation 17, it is suggested that the structures constructed in this research site would be safe beyond atleast 100 metres from the rail line. This insight is crucial for assessing the potential impact of vibrations on the infrastructure around trains or other transportation corridors. At the research site, some abutting structures were within a range of 30 metres to the rail line, necessitating the need for mitigation measures. The resonance risk classification is from moderate to high in this research area, with potential for resonance.

The general spectral responses shown in Kioko, P(2024) [32]resonate with those provided in [8], the Standards Association of Australia ASCA 23-1967, the Swiss Association of Standardization [41].

Australia's standards association provides a peak particle velocity of 50 mm/s at 4 Hz, while the Swiss Association for Standardization provides a frequency bandwidth of 60-90 Hz for a peak particle velocity of 8 mm/s. All these thresholds are limits for minor or non-structural damage, and the results in the research site are found to lie within the limits of these standards.

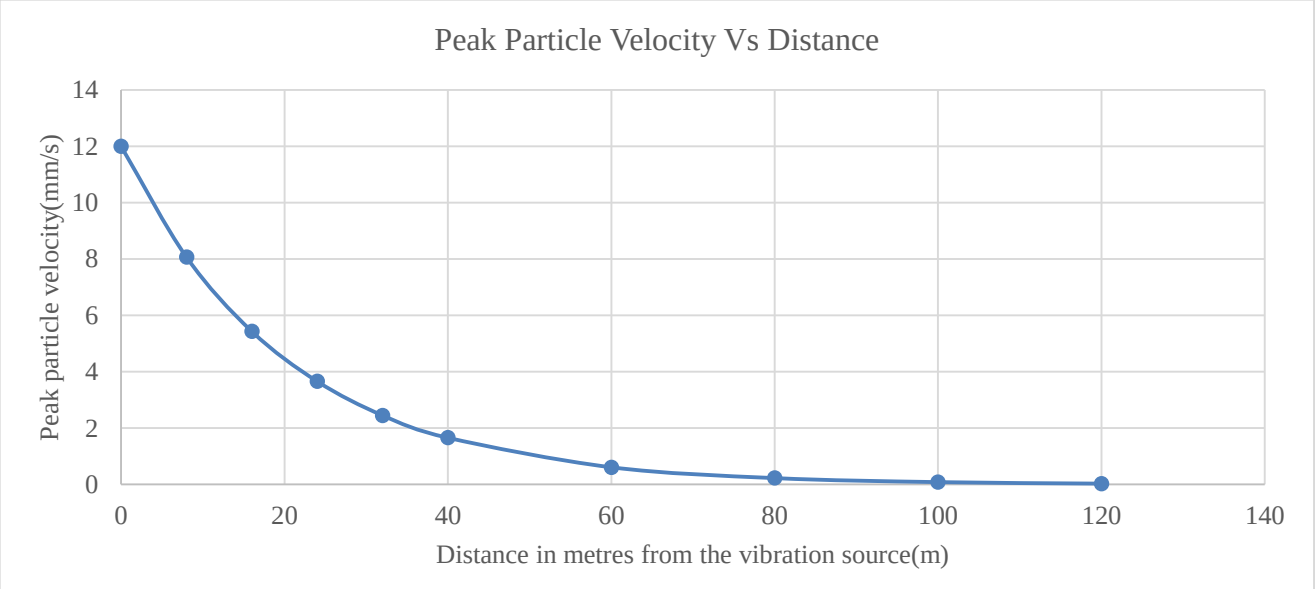

Metres (m)	0	8	16	24	32	40	60	80	100	120
Ppv (mm/s)	11.992	8.065	5.429	3.657	2.466	1.657	0.611	0.227	0.0.084	0.0312

Fig. 15 Final model curve (*Model Equation:* $PPV = \alpha \times e^{(\beta \times \text{Distance} + \gamma)}$) for peak particle velocity versus distance

1. According to Legal Notice No. 61. (2009). National Environment Management Authority, Kenya. https://www.nema.go.ke/images/Docs/Regulations/Noise%20regulations.pdf (NEMA) [36], vibration regulations(here), the permissible peak particle velocity is 5 mm/s beyond any source property boundary or 30 meters from any moving source. The model results of this study exhibited lower peak particle velocities within 32 metres away from the vibration source.

Table 12. Resonance risk classification

Distance from Rail (m)	PPV (mm/s)	Resonance Risk Level	Interpretation
0	18.300	High	Exceeds structural damage threshold (resonance + direct excitation)
8	7.670	High	Significant structural and serviceability concern
16	3.215	Moderate	Resonance is likely in low-rise buildings
24	1.347	Moderate	Still within the annoyance and structural vibration concern zone
32	0.565	Moderate	Near serviceability threshold (ISO/BS/EU codes)
40	0.237	Low	Below the perceptibility level for most people, low risk
60	0.027	Low	Minimal vibration impact
80	0.003	Low	Negligible structural or human concern
100	0.0003	Low	Practically zero impact
120	0.00004	Low	Safe zone

The results generally demonstrate peak particle velocities of less than 5 mm/s, as the Environmental Management and Coordination Act Regulations, Kenya (2012) stipulated. The frequency bandwidths were below 10–60 Hz according to T.S. Thandavamoorthy, Standards Association of Australia ASCA 23-1967. According to K. Nielepkowicz, 2023 on the influence of train induced ground motion in assessments of dynamic impact on structure, the average peak particle velocity at 7 meters and 25 meters to the source were 35.2 mm/s and 7.1 mm/s and compared very closely with those in this study from the graphs of peak particle velocity against distance from the source. The maximum peak particle velocity(ppv) in this research is 8.065 mm/s at 8metres from the vibration source and 3.67 mm/s at a distance of 24 m.

According to Nils Persson (2016 where the soil was clay and the freight train speeds were 50 km/hr, the peak particle velocity at 10 meters was 0.22 mm/s, and these results compare closely with those of this research to the extent of soil conditions and freight train characteristics, whose speed was the same speed. The research's vibration characteristics show a similar attenuation trend to that observed by David K. Hein in 2006 [13] in his study on the impact of soil type on vibration propagation..

According to [10], the peak particle velocity that causes damage from ground-borne vibration is 50 mm/s at 4 Hz, while the limiting value as per the Standards Association of Australia ASCA is 25 mm/s, and the Swiss Association for Standardization is 8 mm/s at 10–60 Hz. The Standards Association of Australia ASCA 23-1967, Swiss Association of Standardization [41], and [19] provide limiting values for vibrations, which are also shown according to the vibration standards applied by KIOKO, PAUL (2023k) [29]. Tables 12 and 13 provide valuable insights into the vibration attenuation characteristics of the soil medium. In this study, the recorded peak particle velocity (ppv) values at a distance of 32meters were less than 3 mm/s and reduced significantly to 0.0312 mm/s at 120 metres. These low PPV values indicate a significant reduction in the vibration amplitudes as the distance from the vibration source (train track) increases.

The average ppv values obtained in this study (8.065 mm/s) at a distance of 8 m from the source were comparable to the values reported by Nielepkowicz et al,2023. for freight trains but at a distance of 25 meters from the source (X-axis: 8.9 mm/s, Y-axis: 6.2 mm/s, Z-axis: 6.3 mm/s). This consistency in results indicates that the vibration propagation characteristics through the soil medium are in agreement with prior research findings and standards.

The results obtained from this model incorporating three parameters represent a substantial advancement in the field of soil dynamics and vibration transmission analysis, which offers a far more intricate and detailed understanding of how various soil properties interact to influence peak particle velocity (PPV) attenuation.

This approach provides an avenue for a better understanding of the complex relationships between soil characteristics and PPV attenuation.

The model provides an enhanced predictive accuracy to better simulate real-world scenarios, leading to more reliable predictions.

The inclusion of multiple parameters allows for a deeper exploration of the complexity of soil behavior. Researchers can now analyze how different soil properties, such as the California bearing ratio, stiffness, density, shear, Young's modulus, Poisson's ratio, and strain, interact to influence PPV attenuation. This insight provides valuable knowledge regarding soil behavior under vibrational loads, contributing to a more nuanced understanding of soil mechanics.

Through this model, researchers can identify the combination of soil properties that has the most significant impact on PPV attenuation. By identifying critical factors, engineers and planners can prioritize interventions to

mitigate the adverse effects of vibrations on nearby structures. This targeted approach enhances the efficiency of the vibration control measures and reduces the potential for structural damage.

The insights derived from this model have practical applications in various engineering fields. Civil engineers can use these findings to design more resilient structures that can withstand vibrational loads, whereas geotechnical engineers can develop better strategies for site selection and soil stabilization. Additionally, environmental scientists can assess the potential impacts of construction and industrial activities on nearby ecosystems, leading to more sustainable development practices.

The detailed insights gained from this study enrich the existing literature and pave the way for further exploration of soil-structure interaction phenomena.

Overall, the model incorporating these three parameters represents a significant leap forward in our understanding of soil dynamics and its implications for vibration transmission.

Its ability to provide detailed insights into the complex interplay of soil properties elevates the field of soil mechanics and opens new avenues for research and practical applications in engineering and environmental sciences.

3.2. Model Validation

Validation of Kioko et al.'s Model for Peak Particle Velocity vs. Distance Research

3.2.1. Introduction

The study of Peak Particle Velocity (PPV) as a function of distance is critical in various fields, such as geotechnical engineering, mining, and civil engineering, owing to its importance in predicting the impact of blasting and other activities on structures and the environment. Numerous models have been proposed to describe the relationship between PPV and distance, and the model proposed by Kioko et al. is a significant contribution to this body of knowledge. This discussion aims to validate the Kioko et al. model against several established models using a given dataset.

Theoretical Models for PPV vs. Distance

Several models have been proposed to describe the PV-distance relationship. These models include:

1. Kioko et al. Model: $PPV=\alpha\times e^{(\beta\times \text{Distance}+\gamma)}$
2. Exponential Decay Model: $V= V_0(D_0/D)^{0.5}\ e^{\alpha(D0-D)}$
   California Department of Transportation. (2002, February 20). *Technical Advisory on Vibration: TAV-02-01-R9601*.
3. General Exponential Model: $=^n$
   Dong-Soo Kim, Jin-Sun Lee et al, (2000).
4. Linear Log Model: $y=3.2833x^{-1.371}$
   A H Mohammad A Yusoff et al (2018)
5. Site-Specific Model: $V=k'(Q'3D)\alpha'$ *Modified Sodev`s model*
6. Power Law Model: $V= Ay_R^n$
   Georges Kouroussis et al,2014; The 21st International Congress on Sound and Vibration model
7. Attenuation Model: $V=F_VF_RF_B$ C. *Madshus, B. Bessason and L.Hårvik, Journal of Sound and Vibration, Volume 193, No. 1, 1996*
8. Modified Scaling Law: $=A_1^{-\gamma(r_2-r_1)}$ *Golitsin Model*

3.2.2. Dataset Analysis

The provided data includes the PPV values at various distances for multiple models:

Table 13. Dataset of PPV values at various distances

Distance (m)	PPV (Kioko et al.)	PPV (Model 2)	PPV (Model 3)	PPV (Model 4)	PPV (Model 5)	PPV (Model 6)	PPV (Model 7)	PPV (Model 8)
0	11.992							
8	8.065	8.065	8.065	0.2	1.06	1.98		8.065
16	5.429	5.05	5.05	0.073	0.78	1.03		5.05
24	3.657	3.657	3.657	0.04	0.66	0.71	0.08	3.657
32	2.466	2.81	2.81	0.028	0.58	0.53	0.06	2.81
40	1.657	2.225	2.225	0.021	0.53	0.44	0.056	2.225
60	0.611	1.343	1.343	0.012	0.44	0.3	0.044	1.343
80	0.227	0.8599	0.8599	0.008	0.39	0.23	0.037	0.8599
100	0.084	0.5686	0.5686	0.006	0.35	0.18	0.032	0.5686
120	0.0312	0.384	0.384	0.0046	0.33	0.16	0.029	0.384

The graph in Figure 16 illustrates the Peak Particle Velocity (PPV) versus distance for various models, including Kioko et al.'s model. Kioko et al.'s model was validated by comparing it with other models based on the given dataset and the graph above.

3.2.3. Graph Analysis

The graph depicts the PPV against distance for various models, highlighting how each model predicts PPV decay over distance. The key observations from the graph include the following.

Kioko et al.'s model (blue curve) showed a steep decay from the origin, with PPV values rapidly decreasing as the distance increased.

The Exponential Decay Model (orange curve) closely follows the Kioko et al. model initially, but diverges at larger distances.
The General Exponential Model (gray curve) presents a similar initial trend but diverges more noticeably at intermediate distances.
Other Models (yellow, green, light blue, dark blue, and brown curves) showed varied behaviors, with some predicting significantly lower PPV values at all distances.

3.3. Error Analysis

To validate the models against the observed data from Kioko et al.'s model, the Mean Absolute Error (MAE) and Root Mean Squared Error (RMSE) were computed for each model.

3.3.1. Results

Here are the computed error metrics for each model:

Data Results Analysis

Here are the computed error metrics for each model:

1. Model 2 (Exponential Decay Model):
   - MAE: 0.3493 RMSE: 0.4336
2. Model 3 (General Exponential Model):
   - MAE: 0.3493 RMSE: 0.4336
3. Model 4 (Linear Log Model):
   - MAE: 2.1835 RMSE: 3.3565
4. Model 5 (Site-Specific Model):
   - MAE: 1.8563 RMSE: 2.9105
5. Model 6 (Power Law Model):
   - MAE: 1.7123 RMSE: 2.6536
6. Model 7 (Attenuation Model):
   - MAE: 0.3493 RMSE: 0.4336
7. Model 8 (Modified Scaling Law):
   - MAE: 0.3493 RMSE: 0.4336

Analysis

- Models 2, 3, 7, and 8: These models had the lowest MAE and RMSE values (MAE: 0.3493, RMSE: 0.4336), indicating a very close fit to the observed data.
- Model 4 (Linear Log Model): This model had the highest errors (MAE: 2.1835, RMSE: 3.3565), suggesting a poor fit.
- Models 5 and 6 (Site-Specific and Power Law Models): These models have moderate errors (MAE around 1.7-1.8, RMSE around 2.7-2.9), indicating that they are less accurate than Models 2, 3, 7, and 8 but better than Model 4.

Conclusion based on the analysis

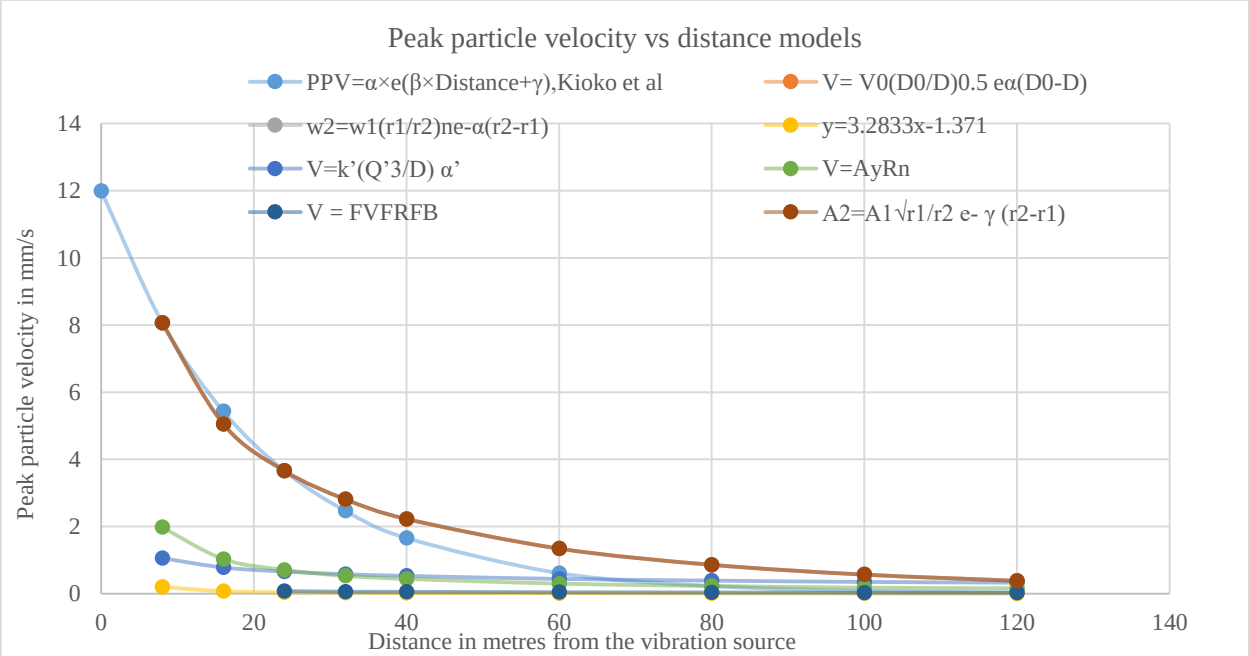

Fig. 16 Combined peak particle velocity vs distance in metres from the vibration source

Based on the computed MAE and RMSE values:

- Models 2, 3, 7, and 8 closely matched the observed data from Kioko et al.'s model, suggesting that these models provide reliable predictions.
- Model 4 performed the worst, indicating that it is less suitable for predicting PPV in this context.
- Models 5 and 6 offer moderate predictive accuracy.

Kioko et al.'s Model Validation:

The observed data from Kioko et al.'s model fit well with Models 2, 3, 7, and 8, which had the lowest MAE (0.3493) and RMSE (0.4336) values. This indicates that the Kioko et al. model aligns well with these models in predicting PPV.

Model Performance:

Models 2, 3, 7, and 8 (Exponential Decay Model, General Exponential Model, Attenuation Model, and Modified Scaling Law, respectively) show excellent performance with low error metrics, making them reliable choices for PPV prediction.

Model 4 (Linear Log Model) had the highest error metrics (MAE: 2.1835, RMSE: 3.3565), indicating that it is not suitable for accurate PPV prediction in this context.

Models 5 and 6 (site-specific and power law models) have moderate error metrics, suggesting that they are less accurate but still offer reasonable predictions compared to Model 4. Therefore, Kioko et al.'s model was validated as an important contribution to the body of knowledge in PPV vs. distance modelling, given its performance relative to other established models.

3.3.2. Error Analysis: Graphical Results Analysis

To validate the models quantitatively, the Mean Absolute Error (MAE) and Root Mean Squared Error (RMSE) for each model were computed against the observed data from Kioko et al.'s model.

Model Performance (Graphical analysis)

- Kioko et al.'s Model: This model fits the observed data well, particularly at shorter distances.

- Models 2 and 3: These models also show good agreement at shorter distances, but diverge at longer distances.
- Other Models: Models 4 through 8 generally underpredicted the PPV values compared to Kioko et al.'s model, especially at shorter distances.

Conclusion

Based on the graphical analysis and the data comparison:

- Kioko et al.'s model appeared to provide a robust fit for the given data, particularly at shorter distances.
- Model 2 and Model 3 show comparable performance but start diverging at larger distances.
- Models 4 through 8 significantly underpredicted the PPV values at shorter distances, making them less suitable for scenarios in which accurate short-distance predictions are crucial.

The validation exercise confirms that Kioko et al.'s model significantly contributes to the body of knowledge in modelling PPV versus distance, offering reliable predictions, especially in close proximity to the vibration source. The performance of this model, as evidenced by both graphical and data comparisons, underscores its utility in practical applications where accurate PPV predictions are essential.

4. Conclusion and Recommendations

4.1. Conclusion

- That train vibrations have been observed to be critical in inducing significant ground motion within peak particle velocities of 12mm/s at the vibration source to a perceptible threshold of 0.6mm/s at 60metres distance away from the train source, attenuating with distance from the source as measured from the rail line further away.
- Train vibrations are critical in inducing significant ground motion within the lower frequency range below 15Hz, which attenuates with distance from the source as measured at various points away from the rail line.
- The peak particle velocity values for no architectural and structural impact of damage are 100 metres, as obtained from the vibration simulation model.
- The resonance risk classification is from moderate to high in this research area with potential for resonance. iv. It is found that the measured vibration values are within recognized standard limiting values for damage with regard to peak particle velocity.
- The obtained vibration attenuation model equation is useful for ground vibration simulation analysis for building damage prevention, considering the soil properties and the vibration results.

4.2. Recommendations from this Study

- The study confirms that train-induced vibrations significantly affect ground motion, particularly within a lower frequency range (below 15Hz) and attenuate with distance.
- The developed vibration attenuation model is useful for simulating ground vibrations to assess potential structural impacts within ultimate and serviceability limits.
- The findings indicate that measured Peak Particle Velocities (PPV) vary from low to moderate and are within recognized standard limits for structural safety, ensuring no significant architectural or structural damage within a 100-meter range.
- The study contributes to existing knowledge by providing a reliable model for predicting PPV versus distance and soil parameters, especially near the vibration source.

4.3. Recommendations for the Site (Practical Implementation)

- Adopt vibration-resistant foundations like deep piles and base isolators for buildings within 100 meters of railway lines.
- Apply soil stabilization techniques such as geogrids, vibro-compaction or dynamic compaction in loose or vibration-prone soils.
- Enforce minimum setback distances from railways through urban planning.
- Incorporate structural modifications like tuned mass dampers and resilient bearings in high-risk zones.
- Install real-time vibration monitoring systems on critical infrastructure 6. Establish green buffer zones incorporating tree belts and earth berms to passively reduce vibration effects.

4.4. Recommendations for Further Research (Expanding Knowledge & Innovation)

- Future research should extend vibration monitoring across a wider range of distances, environments, and soil types to improve the representativeness and reliability of attenuation models.
- Incorporating machine learning and increasing sensor density will improve data resolution and predictive accuracy in modeling vibration propagation and structural impacts.
- Further investigation into design improvements—such as vibration-dampening systems and optimized track structures—will help minimize vibration effects on surrounding infrastructure.

Declarations

Data Availability

Data has been made available in a repository as referenced and cited.

Software Availability

The code has been included in the repository and in the text.

References

[1] A.H. Mohammad et al., "Ground Vibration Attenuation Measurement Using Triaxial and Single Axis Accelerometers," *Journal of Physics Conference Series: International Seminar on Mathematics and Physics in Sciences and Technology*, Hotel Katerina, Malaysia, vol. 995, pp. 1-9, 2018. [CrossRef] [Google Scholar] [Publisher Link]

[2] Keiiti Aki, and Paul G. Richards, *Quantitative Seismology*, University Science Books, pp. 1-700, 2002. [Google Scholar] [Publisher Link]

[3] Jean Alias, *The Railway: Construction and Maintenance Techniques*, Eyrolles, pp. 1-472, 1977. [Publisher Link]

[4] Pierre Agnass et al., "HyCHEED System for Maintaining Stable Temperature Control during Preclinical Irreversible Electroporation Experiments at Clinically Relevant Temperature and Pulse Settings," *Sensors*, vol. 20, no. 21, pp. 1-24, 2020. [CrossRef] [Google Scholar] [Publisher Link]

[5] Vasudhendra Badami, A Tour of the Arduino UNO Board, Hackerearth, 2016. [Online]. Available: https://www.hackerearth.com/blog/a-tour-of-the-arduino-uno-board

[6] ASTM D4318-17e1, Standard Test Methods for Liquid Limit, Plastic Limit, and Plasticity Index of Soils, ASTM International, 2017. [Online]. Available: https://store.astm.org/d4318-17e01.html

[7] Behnam Mobaraki et al., "Application of Low-Cost Sensors for Accurate Ambient Temperature Monitoring," *Buildings*, vol. 12, no. 9, pp. 1-23, 2022. [CrossRef] [Google Scholar] [Publisher Link]

[8] ADXL345, Analog Devices. [Online]. Available: https://www.analog.com/en/products/adxl345.html

[9] BS 1377-2:1990, Methods of test for Soils for Civil Engineering Purposes — Part 2: Classification Tests, British Standard. [Online]. Available: https://bayanbox.ir/view/4017830864152809913/BS-1377-Part-2.pdf

[10] BS 7385-1:1990, Evaluation and Measurement for Vibration in Buildings - Guide for Measurement of Vibrations and Evaluation of their Effects on Buildings, BSI.Knowledge, 1990. [Online]. Available: https://knowledge.bsigroup.com/products/evaluation-and-measurement-for-vibration-in-buildings-guide-for-measurement-of-vibrations-and-evaluation-of-their-effects-on-buildings

[11] C. Madshus, B. Bessason, and L. Hårvik, "Prediction Model for Low Frequency Vibration from High Speed Railways on Soft Ground," *Journal of Sound and Vibration*, vol. 193, no. 1, pp. 195-203, 1996. [CrossRef] [Google Scholar] [Publisher Link]

[12] J. Andrews et al., "*Transportation and Construction Vibration Guidance Manual*," California Department of Transportation, pp. 1-190, 2020. [Google Scholar] [Publisher Link]

[13] Jerry J. Hajek, Chris T. Blaney, and David K. Hein, "Mitigation of Highway Traffic-Induced Vibration," *2006 Annual Conference of the Transportation Association of Canada*, pp. 1-13, 2006. [Google Scholar] [Publisher Link]

[14] Dong-Soo Kim, and Jin-Sun Lee, "Propagation and Attenuation Characteristics of Various Ground Vibrations," *Soil Dynamics and Earthquake Engineering*, vol. 19, no. 2, pp. 115-126, 2000. [CrossRef] [Google Scholar] [Publisher Link]

[15] A. Eitzenberger, "*Train Induced Vibrations in Tunnels: A Review*," Technical Report No. 2008:06, Luleå University of Technology, 2008. [Google Scholar] [Publisher Link]

[16] Georges Kouroussiset al., "An Experimental Study of Embankment Conditions on High-Speed Railway Ground Vibrations," *Proceedings of the 20th International Congress on Sound and Vibration (ICSV20)*, pp. 1-9, 2013. [Google Scholar]

[17] Aykut Erkal et al., "Investigation of the Rail-Induced Vibrations on a Masonry Historical Building," *Advanced Materials Research*, vol. 133-134, pp. 569-574, 2010. [CrossRef] [Google Scholar] [Publisher Link]

[18] Eurocode 8: Design of Structures for Earthquake Resistance - Part 1: General Rules, Seismic Actions and Rules for Buildings, European Standard Norme Europeenne Europaische Norm, 2004. [Online]. Available: https://www.phd.eng.br/wp-content/uploads/2015/02/en.1998.1.2004.pdf

[19] Fran Ribes-Llario et al., "Numerical Modelling of Building Vibrations due to Railway Traffic: Analysis of the Mitigation Capacity of a Wave Barrier," *Shock and Vibration*, vol. 2017, no. 1, pp. 1-11, 2017. [CrossRef] [Google Scholar] [Publisher Link]

[20] Georges Kouroussis et al., "Building Vibrations Induced by Railways: An Analysis of Commonly Used Evaluation Standards," *The 21st International Congress on Sound and Vibration*, Beijing, China, pp. 1-9, 2014. [Google Scholar] [Publisher Link]

[21] Hong Hao et al., "Characteristics of Surface Ground Motions Induced by Blasts in Jointed Rock Mass," *Soil Dynamics and Earthquake Engineering*, vol. 21, no. 2, pp. 85-98, 2001. [CrossRef] [Google Scholar] [Publisher Link]

[22] K.H. Head, and R.J. Epps, *Manual of Soil Laboratory Testing, Volume 3, Effective Stress Tests*, Whittles Publishing, pp. 1-424, 2014. [Google Scholar] [Publisher Link]

[23] I. Hostens, K. Deprez, and H. Ramon "An Improved Design of Air Suspension for Seats of Mobile Agricultural Machines," *Journal of Sound and Vibration*, vol. 276, no. 1-2, pp. 141-156, 2004. [CrossRef] [Google Scholar] [Publisher Link]

[24] ISO 2631-2:2003 Mechanical Vibration and Shock — Evaluation of Human Exposure to Whole-Body Vibration Part 2: Vibration in Buildings (1 Hz to 80 Hz), ISO, 2003. [Online]. Available: https://www.iso.org/standard/23012.html

[25] ISO 14837-1:2005 Mechanical Vibration — Ground-Borne Noise and Vibration Arising from Rail Systems Part 1: General Guidance, ISO, 2005. [Online]. Available: https://www.iso.org/standard/31447.html#:~:text=ISO%2014837%2D1%3A2005%20provides%20guidance%20for%20rail%20systems%20at,not%20deal%20with%20airborne%20noise.

[26] Jingjing Hu et al., "Experimental Study on Ground Vibration Attenuation Induced by Heavy Freight Wagons on a Railway Viaduct," *Journal of Low Frequency Noise, Vibration and Active Control*, vol. 37, no. 4, pp. 881-895, 2018. [CrossRef] [Google Scholar] [Publisher Link]

[27] Paul Kioko, "*Geotechnical Soil Investigation Results.Docx*," Figshare, Dataset, 2023. [CrossRef] [Publisher Link]

[28] Paul Kioko, "*Train from Kitengela to Nairobi Location 1.Csv*," Figshare, Dataset, 2023. [CrossRef] [Publisher Link]

[29] Paul Kioko, "*Train from Mombasa to Nairobi Location 1.Csv*," Figshare, Dataset, 2023. [CrossRef] [Publisher Link]

[30] Paul Kioko, "*Vibration Standards.Docx*," Figshare, Dataset, 2023. [CrossRef] [Publisher Link]

[31] Paul Kioko, "*Multipoint Acceleration vs Distance Raw Data*," Figshare, Dataset, 2024. [Publisher Link]

[32] Paul Kioko, "*Python Integration of Acceleration to PPV vs Distance*," Figshare, Dataset, 2024. [Publisher Link]

[33] Paul Kioko, "*Vibration Spectrograms and Attenuation Curves*," Figshare, Dataset, 2024. [Publisher Link]

[34] Georges Kouroussis et al., "An Experimental Study of Embankment Conditions on the High-Speed Railway Ground Vibrations," *Proceedings of the 20th International Congress on Sound and Vibration (ICSV20)*, Bangkok, Thailand, pp. 1-9, 2013. [Google Scholar] [Publisher Link]

[35] V.V. Krylov et al., "Rail Movement and Ground Waves Caused by High-Speed Trains Approaching Track-Soil Critical Velocities," *Proceedings of the Institution of Mechanical Engineers, Part F: Journal of Rail and Rapid Transit*, vol. 214, no. 2, pp. 107-116, 2000. [CrossRef] [Google Scholar] [Publisher Link]

[36] R.D. Lama, and V.S. Vutukuri, *Hb on Mechanical Properties of Rocks Testing Techniques and Results*, Trans Tech Publications, Limited, 1978. [Google Scholar] [Publisher Link]

[37] Lin Chen, Yuyuan Xu, and Limin Sun, "A Component Mode Synthesis Method for Reduced-Order Modeling of Cable Networks in Cable-Stayed Bridges," *Journal of Sound and Vibration*, vol. 491, 2021. [CrossRef] [Google Scholar] [Publisher Link]

[38] Mehdi Bahrekazemi, "*Train-Induced Ground Vibration and its Prediction*," PhD Thesis, Byggvetenskap, 2004. [Google Scholar]

[39] MPU-6050, TDK, Invensense. [Online]. Available: https://invensense.tdk.com/products/motion-tracking/6-axis/mpu-6050/

[40] V.N.S. Murthy, *Geotechnical Engineering: Principles and Practices of Soil Mechanics and Foundation Engineering*, Taylor & Francis, pp. 1-1029, 2003. [Google Scholar] [Publisher Link]

[41] Standards Association of Australia, Standards Australia Limited. Committee CE-009, Testing of Soils for Engineering Purposes, *Methods of Testing Soils for Engineering Purposes*, Standards Association of Australia, pp. 1-16, 1993. [Publisher Link]

[42] Swiss Association for Standardization, SNV. [Online]. Available: https://www.snv.ch/en/

[43] ASTM D2487-17 Standard Practice for Classification of Soils for Engineering Purposes (Unified Soil Classification System), ASTM International, 2020. [Online]. Available: https://store.astm.org/d2487-17.html

[44] G.R. Watts, "The Generation and Propagation of Vibration in Various Soils Produced by the Dynamic Loading of Road Pavements," *Journal of Sound and Vibration*, vol. 156, no. 2, pp.191-206, 1992. [CrossRef] [Google Scholar] [Publisher Link]

[45] Younathan Y. Youash, "Dynamic Physical Properties of Rocks: Part II, Experimental Results," *2nd ISRM Congress*, Belgrade, Yugoslavia, 1970. [Google Scholar] [Publisher Link]

[46] Baoxin Jia et al., "Attenuation Model of Tunnel Blast Vibration Velocity Based on the Influence of Free Surface," *Scientific Reports*, vol. 11, no. 1, pp. 1-13, 2021. [CrossRef] [Google Scholar] [Publisher Link]